**MINISTRY FOR DEVELOPMENT OF INFORMATION TECHNOLOGIES AND COMMUNICATIONS OF THE REPUBLIC OF UZBEKISTAN**

**TASHKENT UNIVERSITY OF INFORMATION TECHNOLOGIES**

Admit to protection
Chief of TE chair
Ph.D. A.M. Eshmuradov

_____
_____2015 y.

# BACHELOR'S GRADUATIONAL QUALIFICATION WORK

titled: Upgrade of FTTH access networks to OCDMA based solutions

| | | |
|---|---|---|
| Graduator | _____ Signature | Urishov S.A. (name) |
| Advisor | _____ signature | Abdujalilov J.A. (name) |
| SP and LS advisor | _____ signature | Qodirov F. M. (name) |
| Reviewer | _____ signature | _____ (name) |

**Tashkent – 2015**

**MINISTRY FOR DEVELOPMENT OF INFORMATION TECHNOLOGIES AND COMMUNICATIONS OF THE REPUBLIC OF UZBEKISTAN**

**TASHKENT UNIVERSITY OF INFORMATION TECHNOLOGIES**

Faculty Telecommunication technologies chair Telecommunication engineering

Specialization 5522200 - Telecommunication

---

**A P P R O V E D**

Chief of chair TE _____
« ___ »_____ 2015 y.

# A S S I G N M E N T

for the bachelor's graduational qualification work

Sardor Urishov

(name, surname)

titled Upgrade of FTTH access networks to OCDMA based solutions

**1.** Theme is approved be the university order from 25.12.2014 y. №1467

**2.** Deadline for graduational work 31.05.2015 y.

**3.** Source data to work Materials extracted from Internet, books, abstract technical descriptions and equipment User Manuals

**4.** Contents of accounting-explanatory note (list of subjects) 1. Overview of FTTH architectures 2. Overview of optical code division feauteres
3. Implementation of OCDMA in FTTH access network
4.Safety engineering

**5.** The list of graphics material Presentations demo slides

**6.** Delivery date 16.01.2015

Advisor _____
signature

Assignment accept _____
signature

**7.** Advisers on separate sections of graduational work

| Section | Adviser | Signature, date | |
|---|---|---|---|
| | | Assignment given | Assignment taken |
| Chapter 1<br>Chapter 2<br>Chapter 3 | Abdujalilov J.A. | 15.01.2015 y. | 15.01.2015 |
| Chapter 4 | Qodirov F.M. | 23.03.2015 y. | 23.03.2015 y. |

**8.** The schedule of work performance

| № | Section name | Performance date | Advisor signature |
|---|---|---|---|
| 1. | Overview of FTTH architectures | 13.02.2015 y. | |
| 2. | Overview of optical code division multiple access feauteres | 24.03.2015 y. | |
| 3. | Implementation of OCDMA in FTTH access network | 24.04.2015 y. | |
| 4. | Safety engineering | 15.05.2015 y. | |

Graduator _____ «____»_____2015 y.
signature

Advisor_____ «____»_____2015 y.
signature

This graduation thesis is devoted to upgrade of existing FTTH access networks to OCDMA based solutions. In this work, overview of FTTH architectures, OCDMA encoding and decoding and multiplexing principles were studied. During the thesis experimentally demonstrated and incoherent spectral amplitude coding OCDMA have been analyzed.

The thesis also reviewed issues of life safety.

Данная выпускная квалификационная работа посвящена развитию основ решений OCDMA существующих сетей доступа FTTH. В работе рассмотрены принципы построения сетей FTTH, методы кодирования и декодирования OCDMA и способы мультиплексирования. Во время анализа расмотрен анализ OCDMA с способом амплитудного кодирования некогерентного спектра.

В работе так же рассмотрены вопросы безопасности жизнедеятельности.

Ушбу битирув малакавий иши мавжуд FTTH кириш тармоқларини OCDMA ечимлари асосида ривожлантиришга бағишланган. Ишда FTTH тармоғини қуриш усуллари, OCDMA кодлаш ва декодлаш усуллари ва мультиплексорлаш усуллари кўриб чиқилган. Таҳлил давомида когерент бўлмаган спектр амплитуда-кодлаш усули билан OCDMA ни тахлили кўриб чиқилган.

Шунингдек ҳаёт фаолияти хавфсизлиги масалалари ҳам кўрилган.

## TABLE OF CONTENTS

# INTRODUCTION

The role of Telecommunication in Uzbekistan shows the positive growth, and this tendency will proceed. In 2011 our turns grew twice more, and for us it is good indexes. Also as the President of Uzbekistan Islam Karimov adopted the resolution "О мерах по дальнейшему внедрению и развитию современных информационно-коммуникационных технологий" [1] in our country the very great value is attached to development of information communication technologies, in particular, to the direction of software and communication technologies products, providing of infocommunication services for population of Uzbekistan and support of this sphere we see from the government of our republic. The companies cooperate internally in financial, telecommunication, industrial sectors. In the current year the company implemented tens large projects on implementation of the infocommunication services via FTTx PON networks, and also the solution of tasks of infocommunication infrastructure at the largest industrial enterprises of Uzbekistan.

Passive optical networks (PONs) are recognized as an economic and future solution to alleviate the bandwidth bottleneck in the access network [2]. A PON typically has a physical tree topology with an optical line terminal (OLT) located at the root and optical network units (ONUs) connected to the branches. Existing PON standards are based on time division multiplexing (TDM) and can serve up to 32 or 64 users at an aggregate bit rate of 1.25 Gbps [2]. In order to handle future bandwidth demands, many researchers considered wavelength division multiplexing (WDM) to increase the capacity of these existing PONs [13]. However, some limitations to WDM PONs market penetration exist. Adoption of WDM PONs requires upgrading the infrastructure from passive splitters to passive wavelength routers. The use of coherent laser sources in such PONs adds to the cost and complexity of the system, requiring external circuits for laser stabilization. Other solutions which combine subcarrier multiplexing (SCM) to WDM were

proposed to make use of the same wavelength for both uplink and downlink [44]. In this case more electrical circuits containing with local oscillators and mixers are required. Using TDM over WDM PONs helps increase the capacity further, but requires synchronization [40].

Optical code-division multiple-access (OCDMA) combines the large bandwidth of the fiber medium with the flexibility of the CDMA technique to achieve high-speed connectivity [15]. A promising approach for upgrading existing PONs, or for next generation PONs, is the use of OCDMA with its simple ONU and OLT configurations requiring no synchronization [45]. PON infrastructures (i.e., passive splitters) need not to be upgraded to adopt OCDMA. Other attractive features of OCDMA include all-optical processing, truly asynchronous transmission, bandwidth efficiency, soft capacity on demand, protocol transparency, simplified network control, and flexibility on controlling the quality of service (QoS) [15].

In this final qualifying work we focus on incoherent spectral amplitude-coded optical code-division multiple-access (SAC-OCDMA) as a solution for PONs, because of its ability to cancel multiple access interference (MAI), and to permit the use of low speed electronics operating at the bit rate. Furthermore, advances in writing fiber Bragg gratings (FBGs) make possible the design of low cost and compact passive encoders/decoders well adapted to PONs. In our work we examine several PON physical architectures, namely, the use of local sources at each ONU versus the use of a single light source housed at the central office. An inexpensive incoherent light source is placed either at each ONU or at the OLT, for the local sources (LS) architecture or the centralized light sources (CLS) architecture, respectively. In order to manage uplink (from users to OLT) and downlink (from OLT to users) traffic, we consider both two feeder and single-feeder approaches [40].

Much research into OCDMA focuses on optical design, while assuming the availability of high-speed electronics [15]. Emerging research is concerned with the electronic design of receivers for optical multi-access networks, featuring

postprocessing functionalities. Previous electronic receivers were reported in the literature for fast-frequency hop (FFH) OCDMA and PON systems [21]. FFHOCDMA (or λ-t OCDMA) requires electronics that operate at the chip rate rather than the data rate. SAC-OCDMA has the advantage of operating at the data rate, and enjoys excellent MAI rejection with balanced detection. In this work we demonstrate experimentally burst-mode reception of an incoherent SAC-OCDMA PON uplink supporting seven asynchronous users at 622 Mbps (FFH results were at 155 Mbps data rate).

Different PON architectures are tested experimentally, and bit error rate (BER) and packet loss ratio (PLR) are measured. The immunity of the CDR in terms of consecutive identical digits (CID) is also measured. We simulate the BER with FEC in order to validate our measurements. We quantify the increase in soft capacity via FEC, while working with a nonideal recovered clock that provides realistic, achievable sampling. We also present and analyze the cost and power budget (uplink direction) of both LS and CLS SAC-OCDMA PON architectures.

The rest of this final qualification work is organized as follows:

Chapter 1 is concerned with the evolution of PON technology in access network and discusses a number of multiplexing techniques; optical time division multiplexing (OTDM), wavelength division multiplexing (WDM), and optical code division multiplexing (OCDM). Common network topologies will also be discussed with particular emphasis on access networks, both current and future all-optical alternatives.

In the chapter 2, OCDMA encoding/decoding schemes and their enabling technologies are discussed in more detail while also discussing a number of popular optical code sequences. The main OCDMA impairments of MAI and OBN are also presented followed by the main mitigation techniques that are currently used.

Chapter 3 is concerned with the SAC-OCDMA PON physical topologies. We present and compare different OCDMA PON architectures including LS versus CLS architectures, and two-feeder versus single-feeder architectures, and

description of the burst-mode receiver functionalities. The operation of the CDR, CPA, FEC, and the FPGA-based BERT are outlined there. Our experimental setup, as well as the results, are presented and discussed in chapter 3.2. In chapter 3.3, we consider the performance and cost tradeoffs of the LS versus the CLS solution for SAC-OCDMA PONs.

# 1. OVERVIEW OF FTTH ARCHITECTURES

Due to their ultrahigh bandwidth and low attenuation, optical fibers have been widely deployed for wide area networks and metro area networks. To some extent, multimode fibers were also deployed in office buildings for local area networks. Even though optical fibers are ideal media for high-speed communication systems and networks, the deployment cost was considered prohibitive in the access area, and copper wires still dominate in the current marketplace.

In the past few years, various PON architecture and technologies have been studied by the telecom industry, and a few PON standards have been approved by ITU-T and IEEE. FTTx becomes a mature technology in direct competition with copper wires. In fact, large-scale deployment has started in Asia, North America, and Europe, and millions of subscribers are enjoying the benefit of PON technologies.

## 1.1. Evolution of FTTH in access network

Early work of passive optical networks started in 1990s, when telecom service providers and system equipment vendors formed the FSAN (full service access networks) working group. The common goal of the FSAN group is to develop truly broadband fiber access networks. Because of the traffic management capabilities and robust QoS support of ATM (asynchronous transfer mode), the first PON standard, APON, is based on ATM and hence referred to as ATM PON. APON supports 622.08 Mb/s for downstream transmission and 155.52 Mb/s for upstream traffic.

Downstream voice and data traffic is transmitted using 1490-nm wavelength, and downstream video is transmitted with 1550-nm wavelength. For upstream, user data are transmitted with 1310-nm wavelength. All the user traffic is encapsulated in standard ATM cells, which consists of 5-byte control header and 48-byte user data.

APON standard was ratified by ITU-T in 1998 in Recommendation G.983.1. In the early days, APON was most deployed for business applications (e.g., fiber-to-the office). However, APON networks are largely substituted with higher-bit-rate BPONs and GPONs.

Based on APON, ITU-T further developed BPON standard as specified in a series of recommendations in G.983. BPON is an enhancement of APON, where a higher data rate and detailed control protocols are specified. BPON supports a maximum downstream data rate at 1.2 Gb/s and a maximum upstream data rate at 622 Mb/s. ITU-T G.983 also specifies dynamic bandwidth allocation (DBA), management and control interfaces, and network protection. There has been large-scale deployment of BPON in support of fiber-to-the-premises applications.

The growing demand for higher bandwidth in the access networks stimulated further development of PON standards with higher capacity beyond those of APON and BPON. Starting in 2001, the FSAN group developed a new standard called gigabit PON, which becomes the ITU-T G.984 standard. The GPON physical media–dependent layer supports a maximum downstream/upstream data rate at 2.488 Gb/s, and the transmission convergence layer specifies a GPON frame format, media access control, operation and maintenance procedures, and an encryption method. Based on the ITU-T G.7041 generic framing procedure, GPON adopts GEM (a GPON encapsulation method) to support different layer 2 protocols, such as ATM and Ethernet. The novel GEM encapsulation method is backwardly compatible with APON and BPON and provides better efficiency than do Ethernet frames. Deployment of GPON had taken off in North America and largely replaced older BPONs and more. While ITU-T rolled out BPON and GPON standards, IEEE Ethernet-in-the-first mile working group developed a PON standard based on Ethernet. The EPON physical media–dependent layer can support maximum 1.25-Gb/s (effective data rate 1.0 Gb/s) downstream/upstream traffic. EPON encapsulate and transport user data in Ethernet frames. Thus, EPON is a natural extension of the local area networks in the user premises, and connects LANs to the Ethernet-based MAN/WAN infrastructure. Since there is no data

fragment or assembly in EPON and its requirement on physical media–dependent layer is more relaxed, EPON equipment is less expensive than GPON. As Ethernet has been used widely in local area networks, EPON becomes a very attractive access technology. Currently, EPON networks have been deployed on a large scale in Japan, serving millions of users.

Table 1.1.

Comparison of Standardized BPON, GPON, and EPON Parameters

| Parameter | BPON | GPON | EPON |
|---|---|---|---|
| Maximum/ diff. reach | 20 km/20 km | 60 km/20–40 km | 20 km/20 km |
| Maximum split ratio | 128 | 128 | — |
| Linerate (up/down) | 155.52-622.08/155.52–1244.16 Mb/s | 1244.16/2488.32 Mb/s | 1250/1250 Mb/s |
| Coding | NRZ + scrambling | NRZ + scrambling | 8b10b |
| Data rate | Equals the line rate | Equals the line rate | 1000 Mb/s |
| ODN loss | 20/25/30 dB | 20/25/30 dB | 20/24 dB |
| tolerance | 28 dB (best practice) | 28 dB (best practice) | 29 dB (actual systems) |
| US overheads | Fixed 3 bytes Guard: 25.7 ns Guard: 2 μs 154 ns (155.52 Mb/s) | Preamble: 35.4 ns Laser on/off: 512 ns 38.4 ns (622.08 Mb/s) | Delimiter: 16.1 ns AGC/CDR: 400 ns |

Due to its underlying ATM structure, BPON ONUs and OLTs are required to implement ATM switching capabilities. ITU-T G.983 actually specifies OLTs

and ONUs as a whole to function as virtual path (VP) and virtual connection (VC) switches. Moreover, an additional translation between ATM and Ethernet needs to be implemented at the ONU user network interface (UNI) and OLT service network interface (SNI). These complications make BPON equipment unfavorably costly and hinder the growth of BPON systems in a fast-evolving broadband market. Gigabit-capable PON (GPON) is developed to be the next-generation PON technology developed by ITU-T after BPON. GPON is specified such that it can cope better with the changes toward Ethernet and IP communication technologies and meet the fast-growing bandwidth demands. The GPON standard was first rectified by the ITU-T G.984 standard in 2003.

At approximately the same time, the EPON standard was being developed independently by the IEEE standard body to extend basic Ethernet LAN MAC to support new fiber access physical layers. The work of EPON was begun in March 2001 by the IEEE 802.3ah FEM study group and finished in June 2004. Table 1.1 summarizes the operational parameters for BPON, GPON, and EPON standards. As explained earlier, note that all B−, G−, and EPON have converged toward a class B+ type of optics. Class B+ (28 dB ODN loss tolerance) can usually support up to 20 km of reach and a 64 split ratio. The upstream burst overhead for GPON is calculated based on a 1.244-Gb/s bit rate.

## 1.2. FTTH Architecture

Figure 1.1 illustrates the architecture of FTTH based on passive optical network. As the name implies, there is no active component between the central office and the user premises. Active devices exist only in the central office and at user premises. From the central office, a standard single-mode optical fiber (feeder fiber) runs to a 1: N passive optical power splitter near the user premises. The output ports of the passive splitter connect to the subscribers through individual single-mode fibers (distribution fibers). The transmission distance in passive optical networks is limited to 20 km, as specified in current standards. The fibers and passive components between the central office and users premises are

commonly called an optical distribution network. The number of users supported by a PON can be anywhere from 2 to 128, depending on the the power budget, but typically, 16, 32, or 64. At the central office, an optical line terminal (OLT) transmits downstream data using 1490-nm wavelength, and the broadcasting video is sent through 1550-nm wavelength. Downstream uses a broadcast and select scheme; that is, the downstream data and video are broadcast to each user with MAC addresses, and the user selects the data packet–based MAC addresses. At the user end, an optical network unit (ONU), also called an optical network terminal (ONT), transmits upstream data at 1310-nmwavelength.

To avoid collision, upstream transmission uses a multiple access protocol (i.e., time-division multiple access) to assign time slots to each user. This type of passive optical network is called TDM PON. The ONU could be located in a home, office, a curbside cabinet, or elsewhere. Thus comes the so called fiber-to-the-home/office/business/neighborhood/curb/user /premise /node, all of which are commonly referred to as fiber to the x. In the case of fiber-to-the neighborhood/curb/node, twisted pairs are typically deployed to connect end users to the ONUs, thus providing a hybrid fiber/DSL access solution.

When building a FTTH network, it would certainly be important to evaluate what FTTH architectures may be appropriate to adopt. This is important even if it is not related to new developments. However, new developments provide a good opportunity to evaluate and implement the optimal system that is cost effective and satisfies future demands from a FTTH network. Here, we focus on different architectures that are adopted by the FTTH Industry. There are mainly two FTTH architectures that are of current interest, which are namely point-to-point architecture (P2P), and the point to multipoint (P2MP) architectures which are further classified as Active Optical Network (AON), and Passive Optical Network (PON).

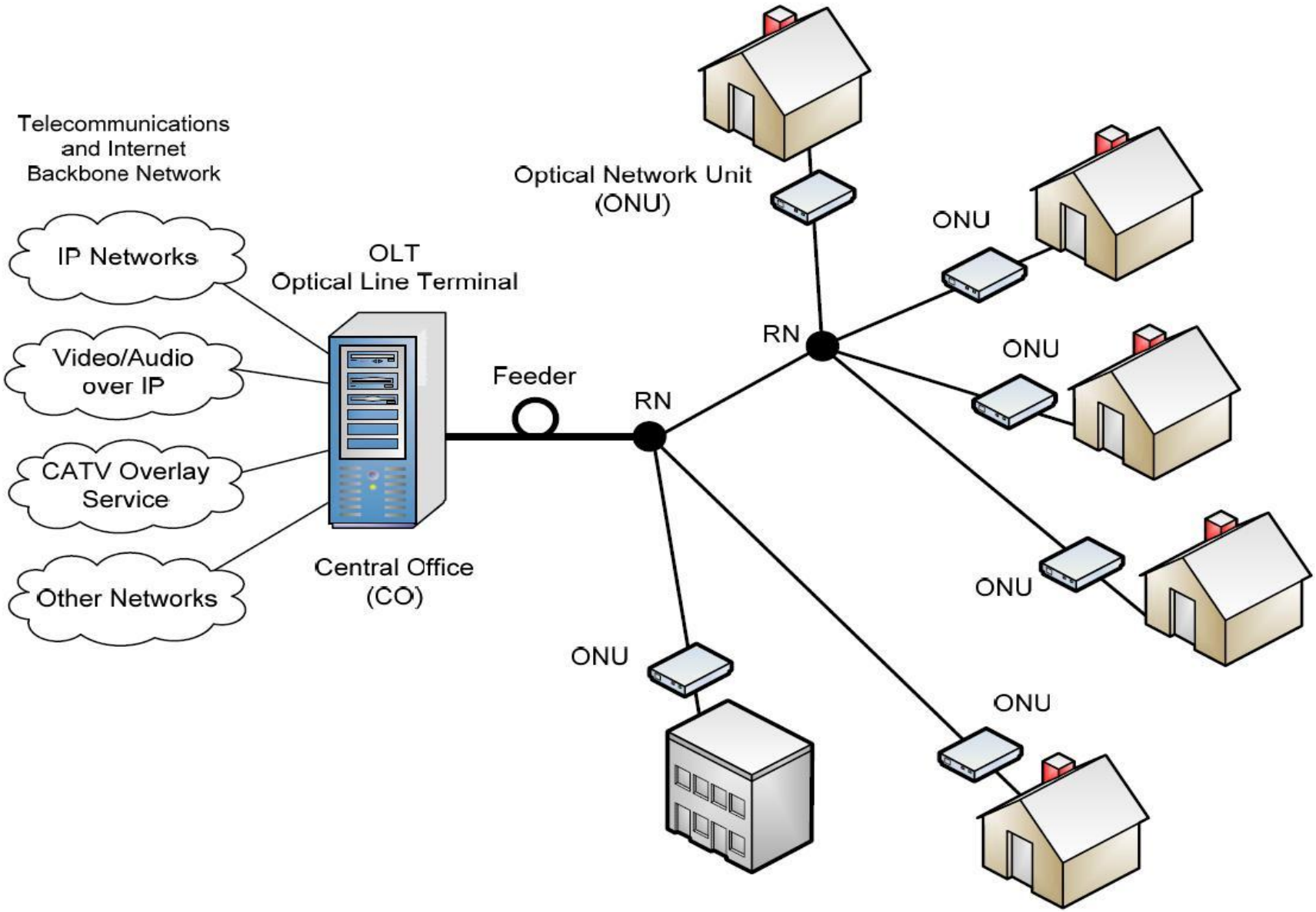


Figure 1.1. Basic architecture of FTTH based on passive optical network

## 1.3. Comparative analysis of multiplexing techniques in PON

While advanced modulation technologies can be used to squeeze out every bit of bandwidth from current legacy networks, this practice can't continue to cope with the increasing demands for bandwidth. Passive optical networks (PONs) are seen as the only viable alternative that can cope with both the capacity demands while also providing these high data rates over transmission distances much larger than those achievable through DSL. In this architecture a feeder fibre runs from the central office to a remote node. This remote node contains a passive optical device that connects the fibre from the central office to the multiple fibres that run to each subscriber. An optical line termination (OLT) in the central office manages the transmissions from each subscriber. At the subscriber end, an optical network unit (ONU) is used to convert the incoming optical signals into the electrical domain. A PON infrastructure can be implemented using a number of schemes; time-division multiple access (TDMA), wavelength-division multiple access (WDMA) or code-division multiple access (CDMA). These schemes make use of the multiplexing techniques discussed in section 1.2 to provide access to the network for users.

**Time-Division Multiple Access PON**

The two most common PON variants which are currently being used in mass roll-outs are gigabit PON (GPON) and ethernet PON (EPON). Both of these networks make use of TDMA PON [29]. A typical TDMA PON layout is shown in Figure 1.5. In these PON infrastructures each subscriber is assigned a dedicated time slot in which they can access the available bandwidth. The passive power splitter couples 1=N, where N is the number of subscribers, of the power from each subscriber into the feeder fibre which is transmitted back to the central office. The OLT at the central office is in charge of assigning the time slots used by each user to ensure that there are no collisions of the data streams. As a result the OLT requires precise time-delay information to each ONU to avoid packet overlap. This is achieved through ranging, however this ranging process needs to be repeated

periodically since the time delays can change over time due to temperature effects on the individual fibres. This process is only important for upstream transmission as the OLT controls how the multiple signals are multiplexed together for downstream transmission.

TDMA PONs also require a burst-mode receiver at the OLT that needs to adjust its clock synchronisation and receiver gain for each transmission from the different subscribers [30].

These receivers can be technically challenging due to the requirement of a wide dynamic range for the different incoming burst signals and a short guard time for the clock synchronization process. In a TDMA PON, unused capacity resulting from some ONUs not transmitting, can be reassigned through dynamic bandwidth allocation, however this adds to the complexity of the control algorithm for the PON. Due to the nature of TDMA PONs, it is believed that they cannot cope with the requirements of future network evolution with respect to aggregated bandwidth and that the insertion losses associated with the splitting ratio will limit the attainable link length [29]. One solution that could mitigate these problems is a WDMA PON.

**Wavelength-Division Multiple Access PON**

In a WDMA PON, similar to that shown in Figure 1.5, each subscriber is assigned a pair of dedicated wavelengths, one for the upstream data and one for the downstream data. This is opposed to a TDMA PON where a pair of wavelengths are shared among the subscribers for the up and downstream transmissions. As a result, each subscriber in a WDMA PON is independent and can transmit at any time without interfering with other channels, eliminating the management issues associated with sharing the network. In comparison to TDMA, WDMA employs a WDM multiplexer, such as an arrayed waveguide grating (AWG), at the remote node instead of a power splitter. An advantage of this is the insertion loss at the node is considerably smaller and independent of the splitting ratio. Another advantage of a WDMA PON is there is no requirement for burst-mode receivers or

a control algorithm to manage transmissions, resulting in simpler network operation. There are however a number of challenges associated with a WDMA PON. Firstly, each ONU requires a wavelength specific source that matches the wavelength profile of the AWG at the remote node. This is difficult to implement in a cost-effective manner as both the wavelength profile of the AWG and the lasing wavelength of the source in the ONU can vary due to environmental changes.

A second disadvantage of a WDM PON is that the OLT requires a separate transceiver for each subscriber. Therefore 2N transceivers are required for the subscribers ONU's and the OLT compared to N + 1 transceivers for a TDMA PON. Despite the difficulties associated with a practical implementation of a WDMA PON, a successful field trail of a WDMA PON has been carried out in Korea [31]. This network uses a broadband light source at the OLT to wavelength lock the Fabry-P´erot (FP) laser in each ONU while also aligning it with the respective wavelength profile of the AWG, mitigating the problem of wavelength drift between the AWG and the ONU laser. Optical comb generation, in which a number of uniform wavelengths are generated a by single laser, has been proposed as a cost-efficient solution to generate the entire wavelength grid using a single source [32]. At the ONU, a shared-source solution has been investigated that aims to eliminate the optical source at the ONU, making it more cost efficient while also reducing the risk of the source wavelength deviating and interfering with adjacent channels. This solution uses a partially modulated signal in the downstream that is split at the ONU with half of the signal remodulated and used in the upstream. A semiconductor optical amplifier (SOA) can be used to both amplify and remodulate the data signal [33]. Although there are a number of challenges to be overcome, it is clear that through field trails and experimental demonstrations, WDMA PON variants have the potential for a unified optical access and backhaul network.

**Optical Code-Division Multiple Access PON**

Since the first experimental demonstration of OCDMA [34] it has been seen as an alternative multiplexing technique to both WDM and OTDM with a number of inherent advantages such as asynchronous transmission, fair division of bandwidth and quality of service control. However, it is only recently that the maturity of all-optical devices required for OCDMA have reached a point where OCDMA can be considered a viable method of transmission in access networks. Device technologies for optical encoding/decoding have demonstrated the ability to encode/decode record length sequences [35], while there has been significant progress in optical thresholding technologies. A typical OCDMA

PON is shown in Figure 1.5. In this network each ONU is assigned a unique optical code that allows them to share the same time slot and bandwidth asynchronously, ideally without interference. As in the case for the TDMA PON, a passive splitter is used at the remote node to combine the individual transmissions onto the feeder fibre back to the OLT. Despite the interest in OCDMA, it has only recently been explored as a technology for PONs with an analysis of a 32-node EPON that uses OCDMA presented in [39]. Although this network used synchronisation, a bit error rate (BER) of less than $1*10^{-9}$ was achievable for all 32 nodes. OCDMA has also been considered for use with a WDMA PON to form a hybrid network for FTTH [40]. In this architecture, OCDMA is overlaid on a coarse WDM (CWDM) system to provide symmetric gigabit channels. This network also takes advantage of the reflection spectrum notches present in the encoder/decoders to suppress WDM interchannel crosstalk. Other promising results have come from a field trial carried out on an 80.8 km link on the Boston-South Network (BOSSNET) [41]. This field trial utilized a compact, integrated multiport AWG-pair encoder/decoder that could support code lengths up to 64 chips. Error-free transmission for two-channels operating at 2.5 Gb/s over 80.8 km without forward error correction (FEC) was demonstrated.

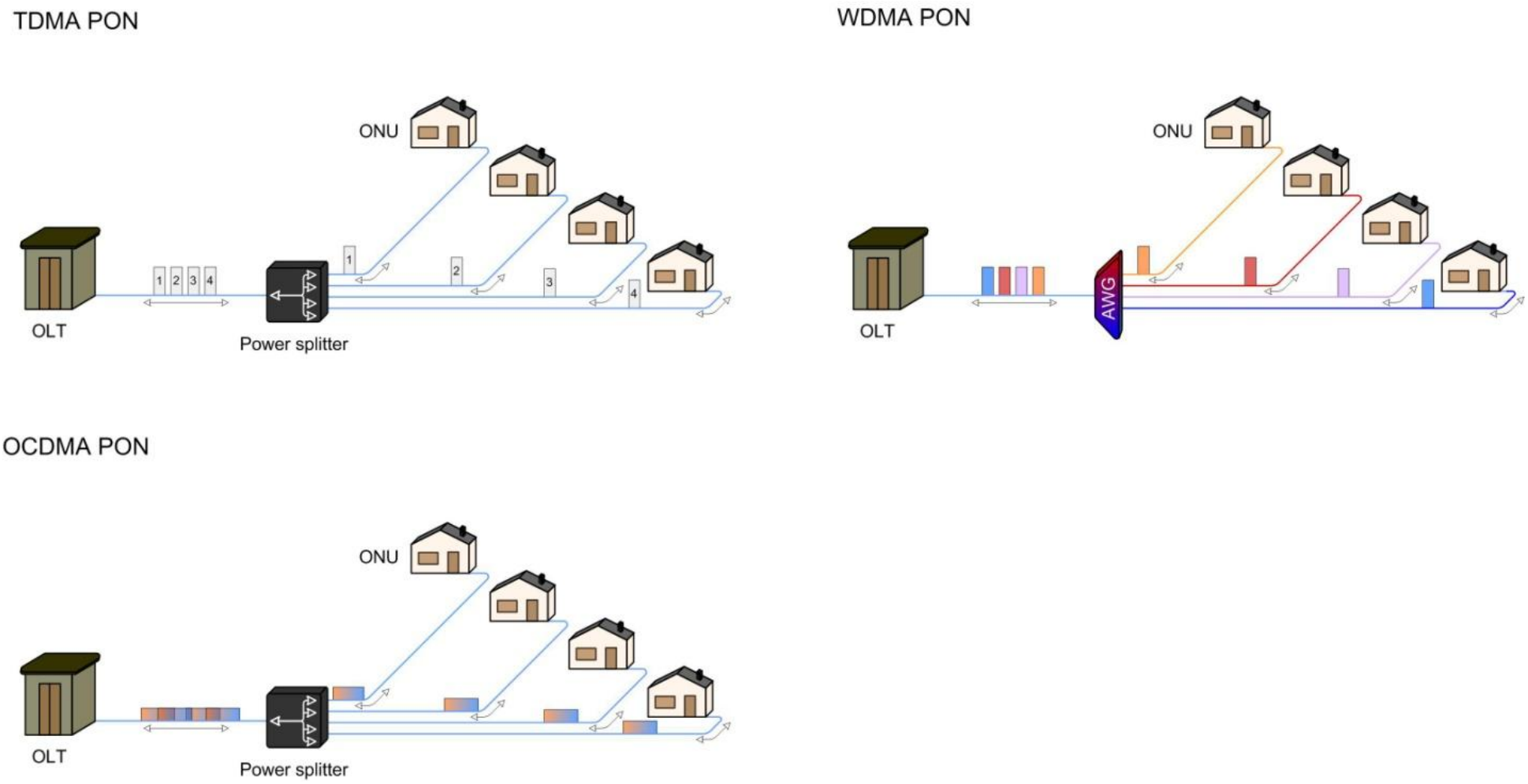


Figure 1.5. Typical layout of TDMA-PON, WDMA-PON and OCDMA-PON.

. The major drawback associated with OCDMA is the presence of multiple access interference (MAI) and optical beat noise (OBN) discussed briefly in section 2.3. These noise sources severely limit the performance of an OCDMA system meaning successful suppression or rejection of both is key to enabling future deployments. One promising technique for the suppression of MAI and OBN is the use of nonlinear effects present in semiconductor devices which could provide a compact, integrated, cost-effective solution for future OCDMA PONs. This technique of noise suppression using semiconductor devices form the main contribution of the work presented in this diploma.

## Summary

The global demand for bandwidth continues to increase at pace with the growth of video and image-based services, HDTV and peer-to-peer services. These services are forcing networks to become more flexible and to accommodate higher bandwidths. While advances in core network technology mean that these networks can handle the increased traffic volume, operational bottlenecks may be shifted to the metro, and in particular the access network. In the next generation of all-optical metro networks, capacity demands will be meet with DWDM. However in the metro and access networks, factors such as cost efficiency, reconfigurability and network complexity become major determinants in the development of these networks. It is envisaged that the final electrical bottleneck in the access layer can be removed by replacing current electrical networks with optical fibre-based technology through deployments such as FTTH. It is widely accepted that these optical access networks will take the form of passive optical networks for their simplicity and cost-effectiveness.

OCDMA is one technique proposed for use in PONs due to its inherent advantages over others. However, it suffers from a number of disadvantages that can also limit the performance of such networks. In this diploma, nonlinear optical devices are presented as a possible solution to these drawbacks that could be used as an compact, integrated and cost-effective solution in future OCDMA PONs.

# 2. OVERVIEW OF OPTICAL CODE DIVISION MULTIPLE ACCESS FEAUTERES

Code division multiple access (CDMA) principles have been investigated in the context of satellite and mobile radio communications since the late 1970's [42]. Since then CDMA has been successfully deployed in cellular telephony networks along with the global positioning system (GPS) satellite broadcast link. The success of CDMA in the wireless domain has inspired research on optical CDMA (OCDMA) with the aim of transferring the inherent advantages associated with CDMA technology to the optical domain. These advantages include flexible access to wide bandwidth, code-based dynamic reconfiguration, decentralized networking, passive code translation and a measure of security through data obscurity [43].

These benefits are particularly advantageous in an optical access network that is required to be flexible, scalable, reconfigurable and cost-efficient. OCDMA technology also allows asynchronous access to each user which is beneficial when considering traffic in an access network tends to be bursty in nature i.e. internet data. As a result, OCDMA provides a more efficient use and fairer division of bandwidth between the users in comparison to other multiplexing techniques.

OCDMA is a spread-spectrum technology where multiplexing is accomplished by encoding each data transmission with an optical code rather than assigning a wavelength of time-slot. This optical code is impressed upon the data to be transmitted with each optical code being unique to a given transmitter. This optical code requires a bandwidth much larger than that required for the transmitted data. As a result, the spectrum of the optical signal is broadened hence the term spread-spectrum. By assigning each transmitting channel with its own unique optical code, OCDMA systems allow all transmitting channels overlap both temporally and spectrally, ideally without interfering. A copy of all transmitted signals added together is passed to all of the receivers. With the knowledge of the code used to encode the desired optical signal, a receiver extracts the desired data

from the aggregate signal by comparing the coded multiuser stream with a copy of the desired code. If the codes match, the original data is recovered while codes that do not match are rejected.

The earliest demonstration of optical CDMA (OCDMA) was given in 1986 [47]. In that experimental demonstration, the CDMA concepts from radio frequency (RF) communications were directly applied to the optical domain using fibre delay lines to construct a temporal coding sequence. Since the publication of that paper, there has been significant progress in OCDMA in terms of the number of coding schemes that have been demonstrated [48] as well as the development of the all-optical technologies that enable such coding operations. New families of optical code sequences were also developed to provide greater discrimination between the desired code and unwanted codes.

Despite the developments in related technologies to date, OCDMA systems suffer from a phenomenon known as multiple access interference (MAI) which limits the overall system performance as the number of active channels increases. MAI arises from the fact that a receiver receives a copy of all transmitted signals and not just the intended signal. Although the decoding operation recovers the desired signal with the remaining unwanted channels improperly decoded, these unwanted channels are still incident on the photodetector resulting in a background noise that scales as the number of users increases. To combat MAI, various optical time gating and optical thresholding techniques have been experimentally demonstrated. Since all users share the same bandwidth, OCDMA also suffers from optical beat noise (OBN) which arises when all the incoming electric fields are mixed in the photodetector. OBN is a severe limitation in OCDMA as it scales with the square of the number of users. Beat noise has been studied in relation to coherent and incoherent OCDMA where it is determined that beat noise can be overcome through the use of a low-coherence source, longer optical codes or through the use of some form of synchronisation.

In this chapter, OCDMA encoding/decoding schemes and their enabling technologies are discussed in more detail while also discussing a number of

popular optical code sequences. The main OCDMA impairments of MAI and OBN are also presented followed by the main mitigation techniques that are currently used.

## 2.1. OCDMA Encoding and decoding

OCDMA is a multiplexing technique where each channel is distinguished by a unique optical code rather than by a wavelength or time-slot. Before transmission each data bit must undergo an encoding operation that optically encodes the data with the desired optical code. At the receiver, the data bit undergoes a decoding process that recovers the original data bit from the optical code sequence. OCDMA systems can be broadly categorized into two areas; incoherent OCDMA and coherent OCDMA. In an incoherent OCDMA system, encoding/decoding typically relies on intensity modulation and uses an incoherent optical source. In comparison, a coherent OCDMA system encodes/decodes the optical signal by manipulating the phase of the optical signal whose source is generally a highly coherent source such as a mode-locked laser. These two broad categories of OCDMA coding are discussed in more detail in the following sections.

### Incoherent OCDMA Coding

In an incoherent OCDMA scheme the encoding/decoding process is based on the summation of optical powers. In the most basic implementation, unipolar codes that are long and sparsely weighted with optical pulses are used. Since the processing is done using the optical power of the pulses, the phase, frequency and spectral content of the codes are not important. As a result, incoherent OCDMA can generally be implemented more easily than coherent OCDMA and can also utilize lower cost wide-band incoherent sources. Incoherent OCDMA can be further divided up into temporal spreading, spectral-amplitude coding, spatial coding and two-dimensional (2D) wavelength hopping/time spreading (WHTS) depending on how exactly the intensity modulated code is applied. In this section

the main incoherent encoding/decoding schemes are discussed in more detail.

### Temporal Spreading Coding

Temporal spreading was the first encoding/decoding scheme experimentally demonstrated for OCDMA in 1986 [47]. In this scheme, each bit period is divided into $N_T$ smaller time intervals, called chips, with $N_T$ being the length of the code used. The optical code is then formed by placing short optical pulses at different chip positions where the number of pulses used in the optical code is the weight of the code. Two examples of these temporally spreading codes are shown in Figure 2.1 (a). A general implementation of a temporal spreading scheme is shown in Figure 2.1 (b) utilizing tapped delay lines and modulators to generate the optical code. Decoding of a temporally spreading optical code is achieved by using the conjugate version of the code in the decoder, which can also be realised using fibre delay lines. In the decoder, the intensities of the chip pulses are summed together at a single chip slot. Time spreading optical codes can be implemented quite easily but are limited due to a number of factors. Firstly due to the fact that processing is performed using optical intensities, long code lengths are required to ensure a satisfactory level of discrimination between the desired and unwanted codes. This requirement for long optical codes sequences leads to a trade-off between optical pulse widths used and the data rate of the channel. If the data rate of the channel is set, meaning the given bit period is a set value, then a longer code must use narrower optical pulses to accommodate the longer code sequence. Conversely, if the optical pulse widths remain constant, then the highest achievable data rate for the channels must drop to allow enough space for a longer optical code.

Temporal spreading OCDMA can be implemented using prime codes [47] or using optical orthogonal codes (OOCs). OOCs are a set of code sequences that are designed to provide the optimal auto- and cross-correlation responses. However, these codes require large code lengths to support a moderate number of users while also using a sparse code weight.

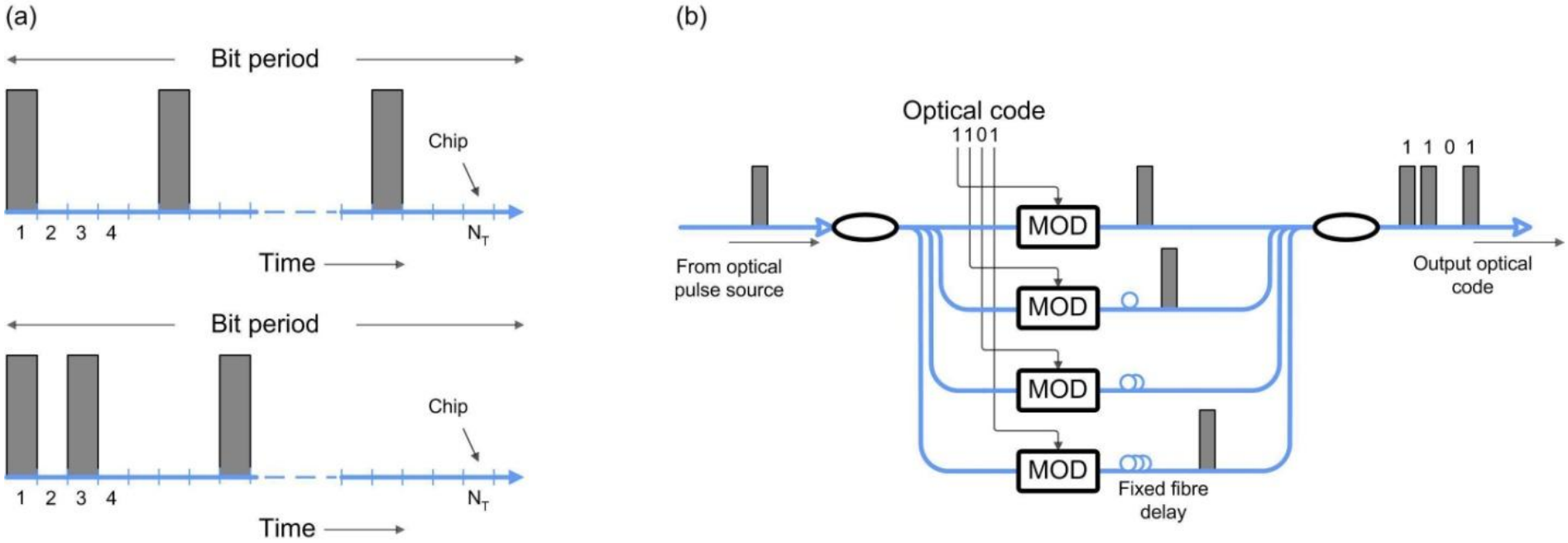


Figure 2.1. (a) Examples of two temporally spread code sequences and (b) One method for the implementation of the code sequences shown in (a). giving an auto-correlation peak representing the original data pulse.

**Spectral Amplitude Coding**

Spectral amplitude encoding (SAE) was first investigated in [49]. In spectral amplitude OCDMA (SA-OCDMA) coding is performed in the wavelength domain rather than the time domain. The advantage of this is that the spectral nature of the codes is decoupled from the temporal nature of the data resulting in the code length being independent of the data rate. This is in direct contrast with time domain coding where the code length used and the highest achievable data rate are connected. The principle of SA-OCDMA is shown in Figure 2.2 (a) where a large broadband spectrum is passed through an amplitude mask that encodes the incoming spectrum according to the given optical code. This spectral mask is divided up into frequency bins that modulate the amplitude of the frequency components. The number of frequency bins that can be resolved by the encoder dictate the code length used. Figure 2.2 (b) shows how this principle can be implemented using a bulk 4-f optical system. A broadband optical source is modulated with the data signal before the frequency content of the signal is spatially dispersed using a uniform diffraction grating and a lens.

The spatially dispersed signal is then amplitude modulated by a suitable mask that contains the optical code. Finally a second lens and diffraction grating are used to recombine the filtered spectrum.

An alternative to using the bulk 4-f system for spectral amplitude filtering is to use fibre Bragg gratings (FBGs) to filter select wavelengths from a broadband spectrum according to a given code. This implementation using FBGs is shown in Figure 2.2 (c). A linear array of FBGs can be used with each one centered at a particular wavelength as designated by the optical code. The reflected spectrum from each FBG in the array corresponds to a ”1” bit in the code with the transmitted spectrum corresponding to the complementary code. However, due to the physical separation of the gratings, the wavelengths will also be separated in time, similar to the effects of chromatic dispersion. One solution is to use an identical array of FBGs but in reverse order to compensate the time delays

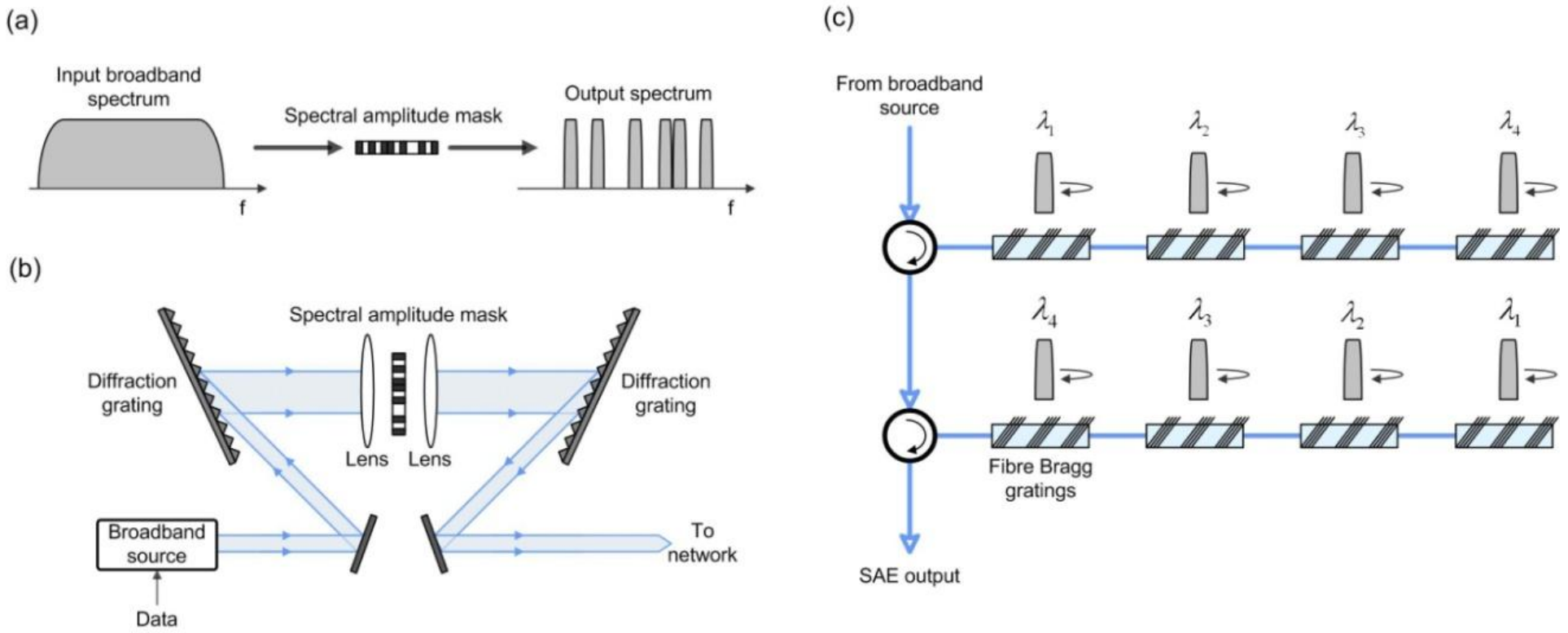


Figure 2.2 (a) SAC principle (b) Implementation of SAC using diffraction gratings and spatial masks and (c) Implementation using fibre Bragg gratings.

incurred. At the receiver, two spectral filters and two photodetectors in a balanced configuration are employed. One of the spectral filters has the same spectral amplitude response as the filter used in the encoder while the second has the complementary response of the optical code. By using specially designed codes in conjunction with balanced detection, MAI can be cancelled.

Experimental demonstrations of SA-OCDMA have shown that eight channels operating at a data rate of 155 Mb/s can achieve bit error rates of less than $1*10^{-9}$ using inexpensive transmitters and without any spectral control. Superimposed FBGs have also been shown to be suitable candidates for encoding/decoding in an SA-OCDMA system [30]. Good MAI rejection was achieved through the use of M sequences and balanced detection. However, the SA-OCDMA system presented still suffered significantly from beat noise limitations that are inherent to this coding scheme.

Wavelength-hopping time-spreading (WHTS) coding, first proposed in [50], is a 2-D scheme where the optical code used is spread in both the time domain and the wavelength domain simultaneously. It is similar to the time-spreading techniques discussed in section 2.1.1. whereby optical pulses are placed at different chip positions according to the given optical code, however in this case these optical chip pulses now have an assigned wavelength. As a result, the encoder essentially creates a combination of two patterns: a wavelength-hopping pattern and a time-spreading pattern. Therefore WHTS codes can be represented as a code matrix with time on one axis and wavelength on the second. Two examples of such codes

are shown in Figure 2.3 (a). The wavelength domain is divided up into $N_\lambda$ channels and the time domain is divided up into $N_T$ chips. A code consists of w short pulses of different wavelength and temporal position, where $\omega$ is the weight of the code. The advantage of using a WHTS OCDMA system comes at the coding level. Firstly, they can exhibit better correlation properties; zero auto-correlations side lobes can be obtained with bounded cross correlations. Also shorter codes are required for good performance in comparison to 1-D schemes.

**Wavelength-Hopping Time-Spreading Coding**

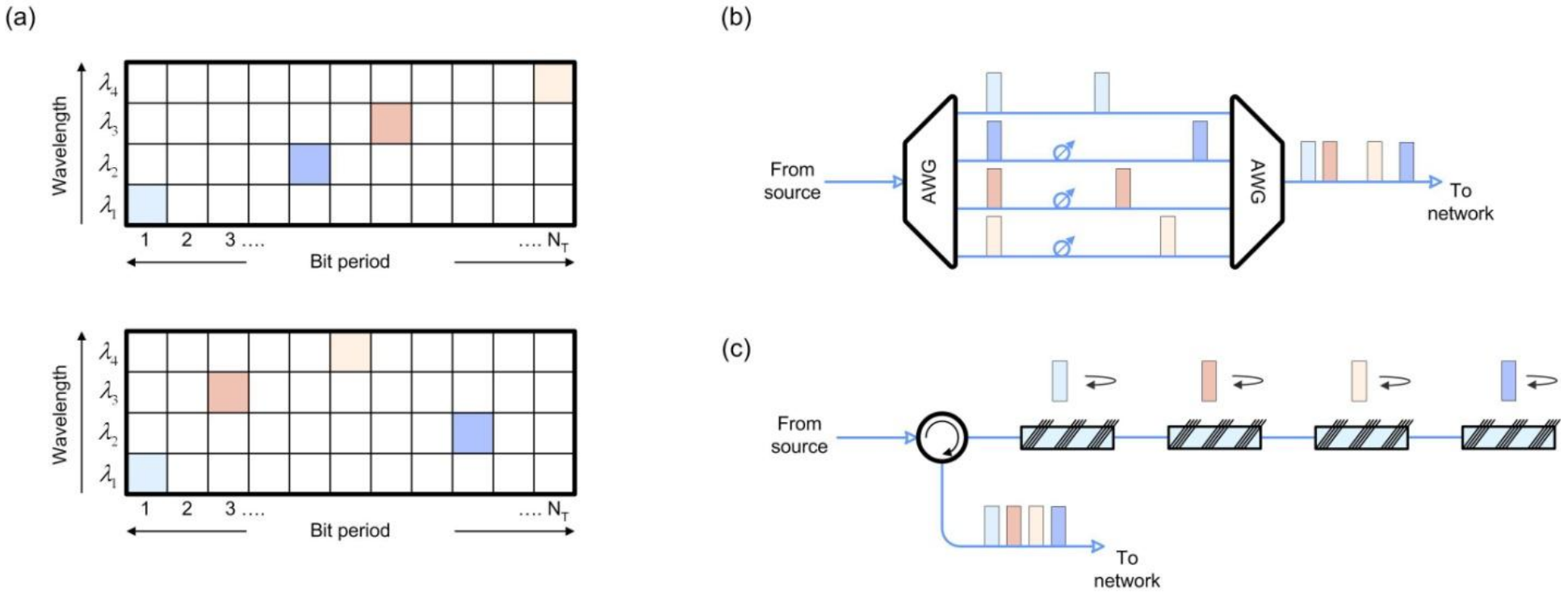


Figure 2.3: (a) Two example codes sequences for WHTS OCDMA (b) Implementation of a WHTS OCDMA encoder using AWGs and tuneable optical delays and (c) using an array of FBGs.

As a result, scalability at higher data rates can be increased as can the number of potential users. A number of technologies have been proposed for encoding/decoding a WHTS OCDMA signal. These include arrayed waveguide gratings (AWGs), FBGs, thin-film filters (TFFs) and holographic Bragg reflectors (HBRs). Figure 2.3 (b) and (c) show two implementations using AWGs and FBGs respectively. Depending on the choice of encoding technology, dynamic variation of the optical codes can be achieved. For example, encoders based on AWGs and TFFs create the desired wavelength-hopping pattern before applying the time-spreading pattern, allowing the use of tuneable optical delays to providing a degree of reconfigurability to the encoders. However encoders based on FBGs and HBRs apply both the wavelength and time patterns simultaneously, preventing independent control of the optical code. The decoder has the same architecture as the encoder with complementary time delays to those used during encoding. During decoding all wavelengths are aligned in time to create an auto-correlation peak of height $\omega$. All unwanted codes remain spread both temporally and spectrally.

Various experimental demonstrations of WHTS OCDMA have been presented in literature. In [36], 16 users, operating at a data rate of 1.25 Gb/s and encoded using FBGs were transmitted over 80 km of fibre. It was shown that the desired channel could be successfully decoded in the presence of interference from the remaining 15 unwanted channels. Error-free operation for a four-channel WHTS OCDMA system, operating at 2.5 Gb/s per channel, was presented in [32]. Encoding was performed using TFFs with a super-continuum spectrally sliced to create the desired wavelength channels. However, an ultrafast all-optical sampling gate was required at the receiver to remove multiple access interference. This demonstration was quickly followed by a 16-user Gigabit ethernet OCDMA system. In this system, each channel operated at 1.25 Gsymbols/s with bit error rates of $1*10^{-11}$ achievable for the correctly decoded signal. Encoding was performed using an AWG and fibre delays. This system also required the use of an optical time gate, in the form of a 13 Gb/s D flip-flop, to suppress MAI. This paper

also describes the significant limitation n that beat noise has on system performance and the number of channels that can be supported.

## Coherent OCDMA Coding

The second category used to classify OCDMA encoding/decoding schemes is coherent OCDMA. In coherent OCDMA an optical code is applied by phase coding the optical field rather than the intensity. Operating on the phase allows the use of bipolar orthogonal codes such as maximal-length sequences and Walsh codes, that result in better system performance due to the close to zero cross-correlations of these types of code sequences. Coherent OCDMA can be divided into temporal phase coding or spectral phase coding depending on whether the coding operation is performed in the time or spectral domain respectively. These two forms of coherent OCDMA are discussed in detail in this section.

The system architecture for temporal phase coding OCDMA is quite similar to that of a temporally spread OCDMA (TS-OCDMA) system. In both cases the bit slot is divided up into $N_T$ chip slots where $N_T$the chip length is. However, unlike TS-OCDMA that generally has a small code weight, a short optical pulse is placed at every chip slot in temporal phase coding. Coding is then performed on the phase of each chip pulse according to the coding sequence used. The applied phase shifts can be simple binary shifts between 0 and $\pi$ or can be more advanced multilevel shifts. Two examples of temporal phase codes are shown in Figure 2.4 (a). In these codes each optical pulse is assigned a $180^o$ phase shift relative to the other pulses. This combination of phase shifts becomes the unique identifier for each channel rather than the position of the pulses within the code sequence. Figure 2.4 (b) shows an implementation of a temporal phase encoder using fibre delay lines and phase modulators. The input pulse is split into N copies which are each phase modulated by an optical phase modulator. Fibre delay lines are then used to align the pulses temporally to form the optical code. The decoder at the receiver follows the same architecture with complementary time delays that realign a number of

**Temporal Phase Coding**

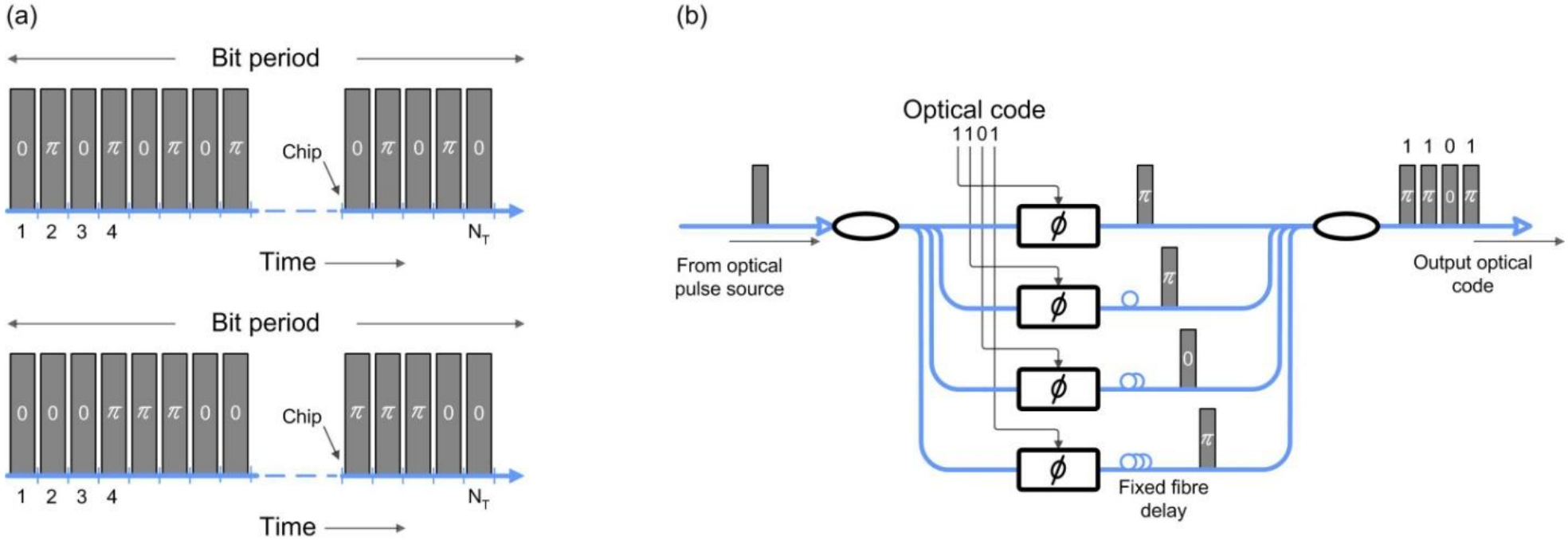


Figure 2.4 (a) Examples of two temporal phase codes (b) Implementation of temporal phase coding using fibre delay lines and optical phase modulators.

optical pulses with the same phase at one chip slot, resulting in an auto-correlation peak. Temporal phase coding for OCDMA systems was originally proposed in using fibre ladder networks. Since then various technologies have been proposed for use with temporal phase coding such as planar lightwave circuits (PLCs) with monolithically integrated tapped delay lines, tuneable taps and optical phase shifters [51], AWG-based multi-port encoder/decoders and superstructured fibre Bragg gratings (SSFBGs) [50]. The longest code lengths to date in OCDMA has been provided by SSFBGs [82]. Both AWG and SSFBGs based encoding schemes have been employed in a large number of experimental demonstrations due to their compact nature and general stability.

Temporal phase coding has received a lot of attention in literature due to its overall superior performance over incoherent OCDMA. In [32], up to ten active channels could be supported while maintaining bit error rates less than $1*10^{-9}$ .Each channel operated at a data rate of 1.25 Gb/s and was encoded using a 511-chip code sequence applied by a SSFBG. A field trial over a 111 km span using a hybrid WDM/OCDMA scheme has also been presented in [41]. The hybrid system employed 10 OCDMA channels each operating at 10.71 Gb/s transmitted over 3 WDM channels. Encoding was performed using a multiport AWG encoder/decoder with DPSK modulation and balanced detection. It is reported that bit error rates lower that $1*10^{-9}$ were achieved with 10 active OCDMA channels on 3 WDM wavelengths. Such a field trial highlights the potential offered by temporal phase OCDMA as a candidate for next-generation networks.

**Spectral Phase Coding**

Spectral phase coding is the second coherent OCDMA technique for encoding data. Spectral phase coding is similar to spectral amplitude coding in that the code sequence is applied to the spectrum of the optical signal. However, as the name suggests, spectral phase OCDMA modulates the phase relationship of the spectrum rather than the amplitude. The operating principle of spectral phase coding is shown in Figure 2.5 (a). A short optical pulse, typically from a mode-locked laser,

is used as the input signal. A mode-locked laser is generally used because it is highly coherent from a frequency perspective; a requirement for a spectrally phase coded system. The spectral content of the optical pulse is then divided into discrete spectral bins with a distinct phase shift applied to each bin. As was the case with temporal phase coding in section 2.1.2., these phase shifts can be binary in nature, such as a 0 or $\pi$ phase shift or they can be a more advanced multilevel format. The spectral phase encoding has the effect of temporally spreading the short optical pulse into a pseudo noise-like signal. The encoded signals from each transmitter are then multiplexed together and sent across the network. The decoder at the receiver is identical in construction to the encoder, the only change is that the spectral phase mask in the decoder is the conjugate of that used in the encoder. When the incoming coded signal and the phase mask in the decoder match, the phase shifts applied to each spectral bin are removed, resulting in the optical pulse temporally reforming to its original state. Figure 2.5 (b) shows the implementation of a spectral phase encoder using diffraction gratings and a spectral phase mask. The architecture of the encoder is identical to the one used for spectral amplitude coding, with the only difference being the mask used to apply the code sequence.

The first successful demonstration of spectral phase OCDMA was presented in [48]. This qualifying work demonstrated that a dispersion-free grating apparatus could be used to disperse the spectral content of a femtosecond optical pulse, allowing a phase code sequence to be applied to the spectrum of the optical pulse. For longer pulses with a reduced bandwidth, such as the bandwidth of a typical WDM channel, the maximum number of chips that can be used may be limited. A virtually imaged phase array (VIPA) has been shown to provide improved resolution ($\sim$1 GHz) in spectral phase OCDMA. While free-space techniques for applying spectral phase codes are useful, a practical system would require a compact, integrated low cost device. As a result, guided-wave devices were investigated for use in spectral phase OCDMA. One example of such a device is a micro-ring resonator, which has been successfully demonstrated as a spectral phase

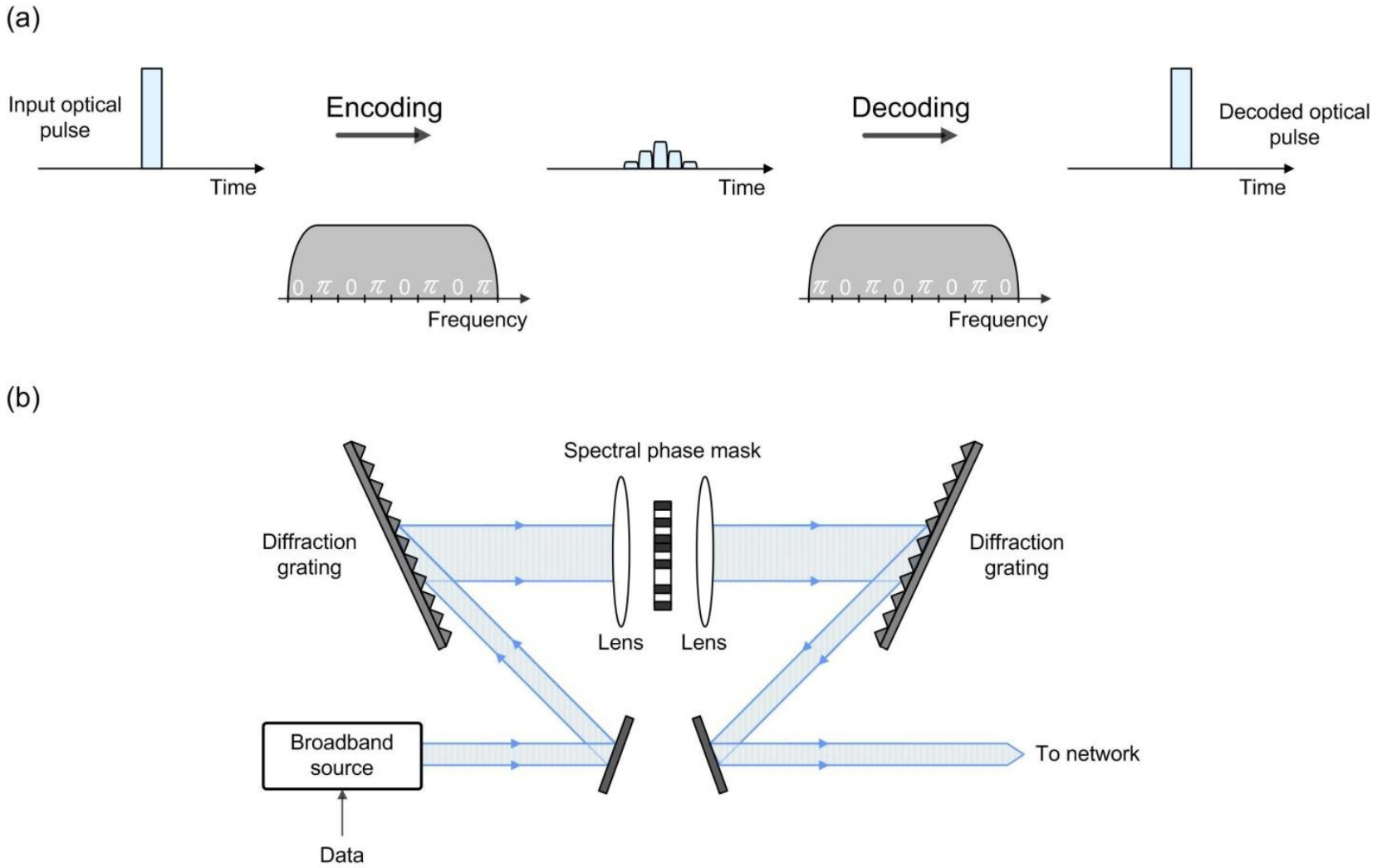


Figure 2.5 (a) Principle of spectral phase coding (b) Implementation using diffraction gratings, lenses and a spectral phase mask.

coder. AWGs fabricated in silica and InP have also been developed for such a purpose. A number of experimental demonstrations of spectral phase OCDMA have been undertaken since its original proposal. In [32], a four channel system operating at 2.5 Gb/s per channel was presented. Each spectral code was applied using a liquid-crystal modulator and a diffraction grating. The paper shows that bit error rates less than $1 *10^{-11}$ could be achieved, however, nonlinear thresholding was required to suppress MAI from the unwanted channels. This experiment also used a slot level coordination scheme to intentionally separate the four users in the time domain to mitigate optical beat noise. A four channel spectral phase OCDMA testbed was presented in [90]. This testbed examined the worstcase scenarios for four channel operation i.e. when all channels are aligned temporally. It is shown that error-free operation was achievable with four simultaneous users, each operating at 10 Gb/s. Again, a nonlinear thresholder was required to suppress MAI. This testbed was later expanded in to 32 channels, each operating at 10 Gb/s. This was achieved by time and polarization multiplexing eight OCDMA channels. By using time-gating, a nonlinear thresholder and forward error correction, bit error rates lower than $1 *10^{-11}$ were possible. The same authors have also demonstrated a two-channel OCDMA link over 80.8 km of BOSSNET in Boston, Massachusetts. The experimental system employed AWG devices to provide the spectral coding. Error free performance was possible for the desired channel in the presence of the interferer through the use of a nonlinear thresholder.

## 2.2. OCDMA Codes

OCDMA is a technique whereby each channel is distinguished by an optical code rather than an assigned wavelength or time slot. Therefore the choice of optical code used is vital to ensure that correct detection of the desired channel is maximized. The choice of the optical code sequence used also has implications for the maximum number of channels that can be supported. Hence the chosen code sequences are ideally orthogonal so that interchannel interference is kept to a

minimum allowing the maximum number of channels to be supported. Optical codes can be divided up into two categories, incoherent and coherent codes, with the choice of code dependent on whether the coding scheme used is incoherent or coherent, as discussed in section 2.1. These two categories can be further divided up according to the code family. The following sections discuss the most common code families that exist for both incoherent and coherent OCDMA.

## Incoherent Codes

In an incoherent OCDMA system, decoding of an optical code sequence is based on the summation of optical intensities. Since optical intensities are unipolar (0; +1) in nature, bipolar code sequences (-1; +1) that have been studied with respect to RF systems may not be optimal in an incoherent OCDMA system. In an incoherent system, the auto-correlation peak is equal to the number of 1's in the code sequence. The peak of the cross-correlation is equal to the maximum number of coincidences of 1's in all shifted versions of the two code sequences [47]. Therefore code sequences that minimize the number of 1's in the code while maintaining a large discrimination between the auto-correlation and the cross-correlation are required. The most common code families used in incoherent systems are prime codes, optical orthogonal codes and carrier hopping prime codes.

### Prime Codes

Prime codes are a set of sequences that have been considered for use in OCDMA networks since the first demonstrations of OCDMA. These codes are time-spread codes that must exhibit a large auto-correlation peak, indicating a matching code at the receiver, and low cross-correlation functions which indicates an incorrect code. The construction of these code sequences are described in [47]. When K users are transmitting simultaneously, the total interference at a given receiver is the superposition of $K-1$ different cross-correlation functions. The

signal-to-noise ratio (SNR) for prime codes is given by [47],

$$SNR \approx \frac{P^2}{0.29(K-1)} \tag{2.1}$$

From equation 2.1 it can be seen that the SNR is directly proportional to the number of chips per code sequence. For a given number of chips, the SNR gradually degrades as the number of simultaneous channels increases. This degradation of the SNR results in an increase in the probability of errors, resulting in poorer system performance for a larger number of users. It has been shown in [57] that to accommodate 31 subscribers on OCDMA system employing prime codes with a probability of error less than $1 * 10^{-9}$ would require a code length of N = 961. This code length severely limits the achievable data rate per channel without placing a strict limit on the optical pulse width of the chip pulses.

**Optical Orthogonal Codes**

Optical orthogonal codes (OOCs), proposed in [31], are a family of (0; 1) sequences with desired auto- and cross-correlation properties that are designed to provide asynchronous transmission and good performance in OCDMA networks. OOCs are designed such that each sequence can be easily distinguished from a shifted version of itself and each sequence can be easily distinguished from a possibly shifted version of every other sequence in the set of codes. In general, an (F, K, $\lambda_a$ $\lambda_c$) optical orthogonal code C, is a family of (0; 1) sequences of length F and weight K where $\lambda_a$ and $\lambda_c$ are the auto and cross correlation constraints respectively. When $\lambda_a$= $\lambda_c$= 1, it has been shown that the number of optical codes is upper-bounded by [56],

$$|C| \leq \left\lfloor \frac{(F-1)}{K(K-1)} \right\rfloor \tag{2.2}$$

where $\lfloor c \rfloor$ the integer portion of the real number x. If an OOC is given by (13; 3; 1; 1) then the maximum number of sequences that can be supported is two, with the two code sequences being,

$$C = \{1100100000000;\ 1010000100000\} \tag{2.3}$$

This demonstrates the main disadvantage associated with OOCs; while the code sequences are designed to provide the maximum auto-correlation while minimizing the cross correlation peaks, this is achieved at the expense of a relatively long code length that supports only a small number of users. It is shown in [33] that for an OOC with a code length of 43 and a weight of three, only seven users can be supported. An extensive treatment of OOCs and their performance analysis is given in [45].

**Carrier Hopping Prime Codes**

Carrier hopping prime codes (CHPCs) are a code family that are used in 2-D wavelength hopping time-spreading OCDMA systems. As described in [36], a $(N_\lambda, N_T, \omega\ \lambda_a, \lambda_c)$ CHPC is a set of $N_T$,* $N_\lambda$ (0; 1) matrices or code words, where $N_\lambda$ is the number of wavelengths and NT is a prime number representing the code length. Each matrix has a weight w with each row of the matrix containing a single 1 element, resulting in each 1 chip in the code being sent on a distinct wavelength. The performance of a multi-wavelength OCDMA system employing $(N_\lambda, N_T, \omega\ 0{,}1)$ CHPCs is examined in [35]. It is shown that the probability that one of the pulses in a signature matrix lining up with a pulse in another signature matrix can be determined. If the decision threshold and the number of simultaneous users is known, then the error probability of a wavelength-time OCDMA system employing CHPCs and hard limiting can be calculated. In general, the error probability can be improved if the number of wavelengths, $(N_\lambda$, and/or the number of chips, $N_T$ are increased. Also CHPCs allow for the adjustment of the number of wavelengths, the number of chips, or both, in order to achieve a given bit error rate performance for a set number of simultaneous users.

**Coherent Codes**

In a coherent OCDMA system, coding is performed by modulating the phase of the optical signal. While a coherent system can be more difficult to implement

than incoherent systems because of the need to provide adequate optical phase control and stability, it offers the ability to implement bipolar codes (-1; +1) that have been shown to have superior performance compared to unipolar codes used in incoherent systems. This performance improvement stems from the autocorrelation peak being equal to $P^2$, where P is the code weight, for coherent systems which is an increase by a factor of P over incoherent systems. The most common code sequences proposed for coherent OCDMA are maximal-length sequences, Walsh codes and Gold sequences.

**Maximal-Length Sequences**

A maximal-length sequence or m-sequence is a pseudorandom sequence that is commonly found in RF and cellular spread spectrum networks. M-sequences are defined as a set of $m$ sequences of length $N = 2^m - 1$, with a detailed discussion on m-sequences is given in [50]. One of the main advantages for using m-sequences is that the correlation function between different shifts of the sequences are always equal to -1, thus allowing them to be used as different codes that have excellent correlation properties. It has been shown that with a relatively short code length, bipolar coding using m-sequences exhibits clear benefits in terms of contrast between the correlation peak and the background, in comparison to unipolar coding [51]. While the number of orthogonal codes for a seven-bit m-sequence is two, this number increases rapidly with code length.

**Walsh Codes**

Walsh codes are a set of code sequences that have been employed in wireless CDMA networks to improve bandwidth efficiency due to their zero cross correlation functions when they are synchronized in time. Walsh functions are generated by mapping codeword rows of special square matrices called Hadamard matrices. These matrices contain one row of all +1's with the remaining rows each having an equal number of +1's and -1's. Walsh codes are defined as a set of N sequences of length $N = 2^n$ and are generated using a recursive procedure. For

example, taking the code set $W_2$, the two code sequences are given by [+1 + 1] and [+1 - 1]. 64-chip Walsh codes have been successfully demonstrated in a 32 channel spectral phase OCDMA network testbed. In this case, Walsh codes were chosen since they are ideally orthogonal signals when used synchronously. Also the MAI produced by Walsh codes ideally does not coincide with the auto correlation peak of the decoded signal but occurs before or after it.

**Gold Sequences**

Gold sequences are a family of bipolar codes that are useful in CDMA networks because of the large number of codes that they supply. A set of N +2 Gold sequences with length $N = 2^m - 1$ can be obtained by using a preferred pair of maximal-length sequences of identical length N. The construction of Gold code sequences is discussed in more detail in [41]. The auto correlation function of a Gold code exhibits side lobes that are dependent on the pair of code sequences used. However, the advantage of using Gold code is that the cross correlation between the codes is bounded. When K users are transmitting simultaneously, the total interference generated is given by the superposition of K - 1 cross correlation functions. Assuming the interferers are uncorrelated, the variance of the total interference is equal to the sum of the variances of the K - 1 cross correlation functions, which are assumed to be identical. It has been shown that the SNR for Gold codes is given by [42],

$$SNR = 4\left\lfloor \frac{N^3}{(K-1)(N^2+N-1)} \right\rfloor \tag{2.4}$$

From this equation it can be seen that the variance of the amplitude of the cross correlation function increases with the both the number of users K and the number of chips N. Therefore, it is apparent that while the number of simultaneous users can be increased by increasing the number of chips per bit, this increase in the number of chips also provides a larger contribution to the overall interference, limiting the improvement in the SNR.

## 2.3. OCDMA network impairments

OCDMA networks can be implemented through various coding techniques and can employ a number of coding sequences which have been discussed in sections 2.1 and 2.2. However, OCDMA networks suffer from two noise sources that can severely limit the number of channels that the system can support. These noise sources are multiple access interference (MAI) and optical beat noise (OBN). The two noise sources arise due to each channel on the network sharing the same bandwidth and time slot equally. Since each channel can transmit asynchronously, two or more channels can overlap in both the temporal and spectral domains. At the receiver, this overlap in both domains results in MAI and OBN. Both noise sources are discussed in more detail in the following sections.

### Multiple Access Interference

Multiple access interference is present in OCDMA systems due to the fact that each receiver receives an aggregate signal that contains the data transmitted from each channel. The optical decoder at the receiver correlates the incoming signal with a stored version of the desired code that is to be detected. The desired channel is decoded correctly and generates an auto correlation peak representing the original data pulse that was transmitted and is detected by the receiver's photodetector. The remaining unwanted channels also pass through the decoder but remain temporally/spectrally spread. However, these unwanted channels are also incident on the photodetector and result in a degradation of the SNR of a desired signal. This degradation scales as the number of simultaneous transmitting channels increases, limiting the performance of the system. The level of MAI has been shown in section 2.3 to be dependent on the length of the optical code used, with longer code sequences performing better due to lower levels of MAI. However, there is generally a trade-off between the practicality of implementing larger code lengths and the level of MAI generated.

An eye diagram similar to that of a correctly decoded OCDMA signal with no interfering channels is shown in Figure 2.6 (a). It clearly shows a large eye opening that allows the decoded data to be successfully thresholded and recovered. In comparison, Figure 2.6 (b) shows the same decoded channel, this time in the presence of an interfering channel. This interfering channel introduces a third intensity level to the eye opening that effectively reduces the 'correct' portion of the eye opening, increasing the probability of error after detection. Both optical signals in Figure 2.6 were detected using 50 GHz photodiode, hence there is a clear distinction between the correctly decoded optical pulse, that has a narrow pulse width and high optical peak power, and the incorrectly decoded MAI that is spread over the entire bit slot and has a low optical peak power. However, the energy in both the desired and unwanted channel is the same, with both signals having a temporal duration that is equal to or below the bit period, meaning that they appear essentially identical to a photodetector that is band-limited to the data rate. This would result in a three-level eye diagram and an optical signal that cannot be correctly recovered without errors since the band-limited receiver cannot distinguish between the desired channel and the interfering channel. Consequently, either a fast receiver that has a bandwidth greater than the data rate of the desired channel must be used, or some form of optical thresholding or time gating is required to remove MAI.

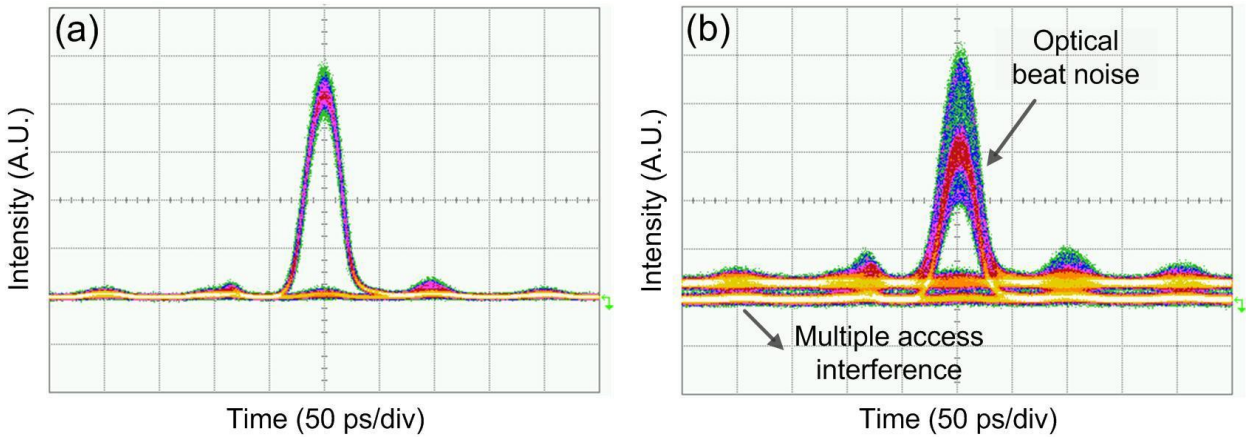


Figure 2.6. Output pulses from an OCDMA decoder for (a) Single correctly decoded channel (b) Correctly decoded channel with MAI and optical beat noise.

## Optical Beat Noise

Optical beat noise is the second major impairment to OCDMA networks. Beat noise arises when different optical signals with identical (or nominally different) frequencies are incident on a given photodetector simultaneously. Since a photodetector has a square-law detection characteristic, optical beating will occur between the optical signals incident on the detector. When two optical signals are incident on a photodetector, the total intensity, $I$, is given by [44],

$$I = I_1 + I_2 + 2\sqrt{I_1 I_2}\cos(\delta\phi) \tag{2.5}$$

where $I_1$ and $I_2$ are the intensities of the two optical signals and $\delta\phi$ is the phase difference between the two signals. From equation 2.5 the total intensity can beat from a minimum value of $I_{min} = I_1 + I_2 - 2\sqrt{I_1 I_2}$, if the two waves are out of phase, to a maximum of $I_{max} = I_1 + I_2 + 2\sqrt{I_1 I_2}$, if the two waves are in phase. This variation in the intensity of the optical signal can severely degrade the performance of an OCDMA system.

Figure 2.6 (b) highlights the intensity variation caused by optical beating between two OCDMA signals. It can be seen that OBN introduces a large amount of noise to the top of the eye diagram in comparison to the single channel eye diagram shown in Figure 2.6 (a). The limits on the performance of OCDMA systems as a result of OBN are often larger than those resulting from MAI. This is due to beat noise scaling with the square of the number of detected fields, which is proportional to the number of channels [45]. These include reducing the level of interference between the OCDMA channels through either using a longer code sequence or introducing some form of synchronisation to the system. Implementing a longer code sequence can increase hardware cost and/or limit the transmission data rate depending on the OCDMA scheme employed. Introducing synchronization to the system has the effect of lowering the bandwidth efficiency and increasing the overall complexity of the network. A second option is to use a low-coherence source such as a wide-band light emitting diode (LED) or amplified spontaneous emission (ASE). Such a solution can be effective in an incoherent

OCDMA system at reducing beat noise but is not suitable for a coherent system that requires an optical source that has a coherence length of at least the chip length.

## Summary

Optical code division multiple access is a promising multiplexing technique that is particularly suited for future all-optical access networks. OCDMA has a number of inherent advantages such as asynchronous transmission, quality of service control and a large degree of flexibility and scalability. Various demonstrations of enabling technologies have been presented in literature allowing a number of different OCDMA coding techniques to be achieved. These include coding in both the temporal and spectral domains, or through a combination of both. Coding can either be performed on an amplitude or phase basis with advantages and disadvantages associated with both. However, all OCDMA systems suffer from two main impairments that limit the overall system performance, multiple access interference and optical beat noise. Both noise sources scale with the number of simultaneous users, resulting in the need for some form of rejection and/or suppression to ensure that a given performance level can be achieved.

## 3. IMPLEMENTATION OF OCDMA IN FTTH ACCESS NETWORK

In this final qualifying work, we demonstrate experimentally the uplink of a 7×622 Mb/s incoherent spectral amplitude coded optical code-division multiple access (SAC-OCDMA) passive optical network (PON) with burst-mode reception. We consider two network architectures: local sources (LS) at each optical network unit (ONU) versus a single source located at the central office. We examine both architectures over a 20-km optical link, as well as a reference back-to-back configuration. Our architectures can adopt two feeder and single-feeder topologies; however, we only test the two-feeder topology and therefore the effect of Rayleigh backscattering is neglected. We also study the relative merits (cost and performance) of local sources versus centralized architectures. A penalty of less than 2 dB between the LS and the centralized light sources (CLS) architectures was measured at a bit error rate (BER) of $10^{-9}$ under certain assumptions on the relative power of the sources. The power budget in the CLS architectures is more critical than in the LS architectures; extra splitting and propagation losses exist as the uplink travels through the network back and forth. Doubling the number of users while maintaining the same distance and source power in LS architectures imposes 3-dB additional losses, whereas for CLS architectures, there are 6-dB extra losses. CLS architectures can overcome these penalties using amplification at the central office. Alternately, central office amplification can be used to more than double the number of users in LS SAC-OCDMA PONs. A standalone (no global clock) burst-mode receiver with clock and data recovery (CDR), clock and phase alignment (CPA), and Reed-Solomon RS(255,239) forward-error correction (FEC) decoder is demonstrated. A penalty of less than 0.25 dB due to the nonideal sampling of the CDR is reported. The receiver also provides an instantaneous phase acquisition time for any phase step between consecutive packets, and a good immunity to silence periods. A coding gain of more than 2.5 dB was reported for a single-user system, and BER floors were completely eliminated. Error free transmission (BER $< 10^{-9}$) for a fully loaded PON was achieved for the LS architecture as well as the

CLS architecture. Continuous and bursty upstream traffic were tested. Due to the CPA algorithm, even with zero preamble bits we report a zero packet loss ratio (PLR) for up to four simultaneous users in case of bursty traffic, and more than two orders of magnitude improvement in the PLR for fully loaded PON systems.

## 3.1. SAC-OCDMA PON Architectures

Tree architectures are widely used for fiber-to-the-home (FTTH), or the so called “last mile” market. Such networks referred to as PONs employ only passive components (couplers, circulators, etc.) in the optical distribution network (ODN) and at the remote node (RN), and they have low installation and management costs. Different PON architectures have been proposed by different research groups [102, 103], including both two-feeder and single-feeder architectures to multiplex uplink and downlink traffic. In two-feeder architectures, uplink and downlink traffic is sent independently on separate feeders; a single-feeder architecture carries both uplink and downlink on one fiber. Although single-feeder topologies reduce infrastructure and maintenance costs, they suffer from Rayleigh backscattering if the same wavelength is used for upstream and downstream. Two-feeder architectures give the flexibility to use the same wavelength band for upstream and downstream, making the design easier.

Although our OCDMA PON architectures offer the flexibility of adopting both twofeeder and single-feeder architectures, we test only the two-feeder architecture for experimental convenience. The effects of Rayleigh backscattering, which are reduced in such architectures, are then not addressed.

In this final qualification work, we propose four different architectures for SAC-OCDMA PONs as illustrated in Figure 3.1; both LS architectures [Figure 3.1(a)] and CLS architectures [Figure 3.1(b)] can exist with two-feeder and single-feeder topologies (shown within the ODN). We analyze both architectures with each feeder topology in terms of power budget, but we experimentally test only the two-feeder topology. Although our architectures provide full-duplex communications,

we focus on the design of the ONU side, as it is one of the most challenging factors in PON design. More specifically, we focus on the design of the ONU transmitter (uplink transmitter). The optimum receiver for a SAC-OCDMA PON at both the OLT and ONU is the conventional balanced receiver because of its ability to suppress first-order MAI. The structure of such a receiver for the ONU is given in Figure 3.1, including a 1×2 coupler, a decoder (DEC), a complementary decoder ( DEC ) , and a balanced photodiode (PD). Fiber Bragg gratings working in transmission are used as the encoders/decoders because

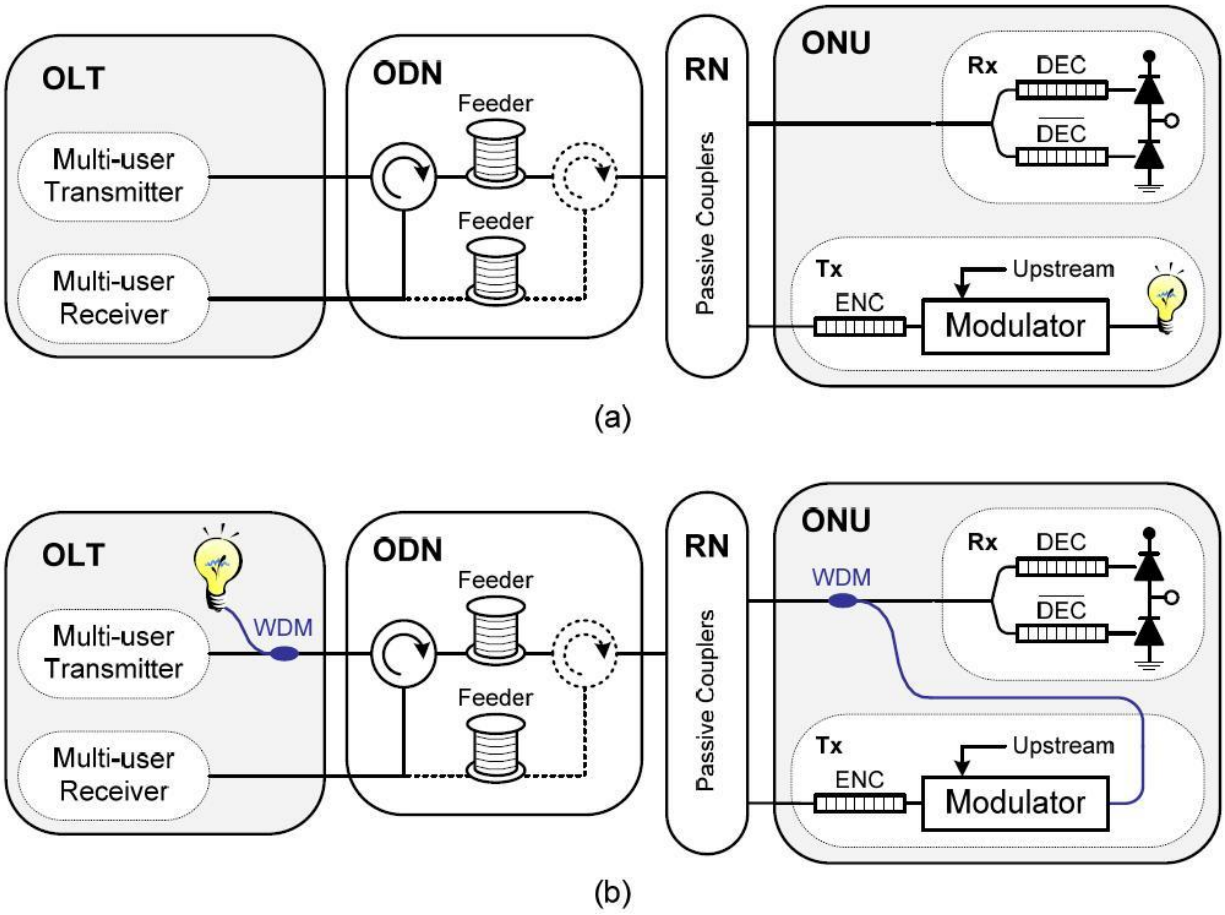


Figure 3.1. SAC-OCDMA PON physical architecture: (a) LS architecture, (b) CLS architecture.

of their good group delay performance, which is vital in SAC-based OCDMA systems [105]. Figure 3.1(a) shows the proposed LS SAC-OCDMA PON; in that case, an inexpensive directly modulated light emitting diode (LED) or a broadband erbium-based source is externally modulated and located at each ONU. On the

other hand, the proposed CLS SAC-OCDMA PON, shown in Figure 3.1(b), places a single powerful source at the OLT with remote external modulation of that source at each ONU. In CLS architecture, coarse WDM filters are needed at the OLT and ONU, as shown in Figure 3.1(b), to separate the continuous wave light for the uplink from the modulated downlink. Such filters can be replaced by passive couplers if the same wavelength band is used for both downlink and uplink. The RN, the ODN, and the OLT multiuser transmitter/receiver are similar for the two architectures. The RN consists of passive combiners and splitters, as in existing TDM PONs, so there is no need to upgrade the PON infrastructure; for WDM PONs, the couplers must be replaced by arrayed waveguide gratings (AWGs). The RN serves as a connection between the ONUs and the ODN. Users are connected to the RN through short length fibers (~1 km) called distribution drop fibers. The ODN, composed of feeder fibers (~20 km) and passive optical circulators, can adopt a two-feeder (the second feeder with its corresponding circulator shown in dotted in Figure 3.1) or a singlefeeder architecture. At the OLT, a multiuser transceiver is used to communicate with all the users in both directions. The OLT should contain optical amplifiers to compensate for the losses through the network and also for the combining and splitting losses of the multiuser transmitter and receiver when implemented all optically (the same design as ONUs in Figure 3.1). Note that electronic implementation of OLT transceivers could help reduce the loss budget significantly by eliminating the optical couplers. Furthermore, all preprocessing and postprocessing functionalities could be easily handled in electronics. The uplink power budget of the proposed PON architectures in Figure 3.1 is mainly affected by the RN and the ODN adopted. In LS architectures [see Figure 3.1(a)], the uplink signal travels only in one direction, from the ONU to the OLT. For N ONUs (corresponding to a 1:N splitting ratio), we have 10log(N) dB splitting losses, in addition to the propagation losses through one feeder and the insertion losses of a three-port circulator. These observations are valid for both the two-feeder and the single-feeder topology. In the CLS architecture, shown in Figure 3.1(b), for uplink, the unmodulated source travels

from the OLT to the ONU and after modulation returns to the OLT. Therefore, a CLS PON experiences twice the ODN and RN losses (splitting losses + propagation losses + insertion losses) as a similar LS PON, again whether the two-feeder or the single-feeder topology is used. We will discuss in Section V the performance and cost tradeoffs of the LS versus the CLS solution.

## SAC-OCDMA Burst-Mode Receiver

According to the PON standards, a continuous downlink in the wavelength band of 1480-1500 nm carries TDM data, or OCDMA encoded data in our case, from the OLT towards multiple ONUs. A burst-mode link in the 1310-nm window collects all ONUs upstream traffic toward the OLT as variable-length packets at the same rate. Because of the bursty nature of the upstream, the OLT receives packets from active ONUs with different amplitude levels and phases. In class B PONs, the average signal level may vary 21 dB in the worst case from packet to packet. These packets are of variable length and are interleaved with a guard time of only four bytes as specified by the physical medium dependent (PMD) layer.

A typical burst-mode uplink signal that complies with PON standards is used as a test signal in our experiments and is shown in Figure 3.2(a). Packet 1 serves as a dummy packet to force the burst-mode CDR to lock to a certain phase ( $\varphi_1$) before the arrival of packet 2. A silence period including m CIDs and a phase step $\Delta\varphi$ is inserted between the two packets. This idle period also represents the asynchronous nature of OCDMA due to the random phase step $-2\pi \leq \Delta\varphi \leq +2\pi$ between the two packets. The PLR measurements and their corresponding BER measurements are performed only on packet 2, which consists of preamble bits, 20 delimiter bits, $2^{15}$-1 payload bits, and 48 comma bits. The preamble and the delimiter bits correspond to the physical layer upstream burst-mode overhead at 622 Mb/s, as specified by the ITU-T G.984.2 standard [51]. The preamble bits are used to perform phase recovery. The delimiter is a unique pattern indicating the start of the packet to perform byte synchronization.

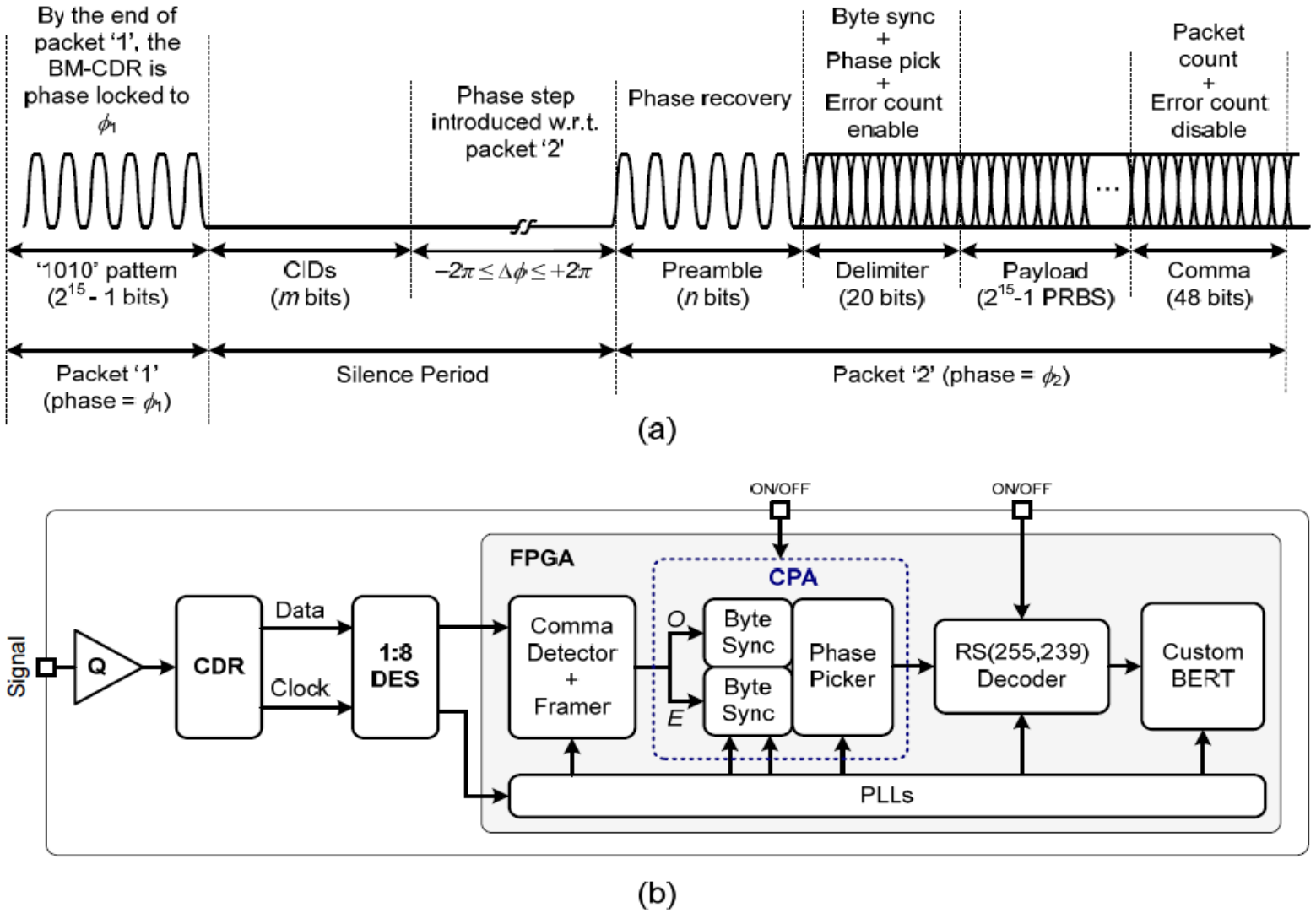


Figure 3.2. (a) Typical burst-mode uplink test signal used to test the phase acquisition time of the clock phase aligner, (b) block diagram of the OLT burst-mode receiver for SAC-OCDMA PONs (DES: deseria lizer, Sync: synchronizer).

binary sequence (PRBS). The BER and PLR are measured for the payload bits only. The lock acquisition time corresponds to the number of bits (n) in front of the delimiter in order to get a zero PLR for over 3 min at 622 Mb/s (>106 packets received, i.e., PLR<$10^{-6}$), a BER<$10^{-10}$, and for any phase step ($-2\pi \leq \Delta\varphi \leq +2\pi$) between consecutive packets [100]. We will demonstrate that even at n = 0, i.e., no preamble bits, our phase picker gives excellent results. To generate alternating packets with adjustable phase, as in Figure 3.2(a), we combined two programmable ports from the HP80000 pattern generator shown in Figure 3.3 using a radio frequency (RF) power combiner. The phase steps between the consecutive packets can be set anywhere between ±2 ns on a 2 ps resolution, corresponding to a ±1.25 unit interval (UI) at 622 Mb/s. Note that 1 UI corresponds to 1-bit period.

## Building Block Diagrams

The main building blocks of the SAC-OCDMA burst-mode receiver we designed are illustrated in Figure 4.2(b). The receiver includes a multirate SONET CDR from Analog Devices (Part #ADN2819), a 1:8 deserializer from Maxim-IC (Part #MAX3885), and a CPA module and a FEC RS(255,239) decoder implemented on a Virtex II Pro FPGA from Xilinx. Our receiver without the CPA is therefore similar to that in [51], but without the return-to-zero (RZ) to nonreturn-to-zero (NRZ) converter needed for FFH-OCDMA. The receiver also avoids the use of an 8:1 serializer (used with FFH-OCDMA) to up convert the frequency. The quantizer (Q) is used before the CDR to threshold the incoming signal to filter out intensity noise and other channel impairments. The threshold is manually adjusted to sample in the middle of the eye opening to obtain the optimum BER. The multirate CDR then recovers the clock and data from the incoming signal. The receiver is operated at either 622 or 666.43 Mb/s depending on whether the FEC module is OFF or ON, respectively. The CDR is followed by a 1:8 deserializer (DES) that reduces the frequency of the recovered clock and data to a frequency that can be processed by the digital logic. Afterwards, a framer, a comma detector,

a CPA (including a phase picker and byte synchronizers), phase locked loops (PLLs), an RS(255,239) decoder, and a custom BERT are implemented on an FPGA. Note that a computer is used to control the output of the pattern generator and to communicate with the FPGA on the receiver (Figure 3.3). Automatic detection of the payload is implemented on the FPGA through a comma detector and a framer, which are responsible for detecting the beginning (delimiter bits) and the end (comma bits) of the packets, respectively, as in [51]. The CPA module makes use of the phase picking algorithm in [108] and the CDR operating at 2× oversampling. The CPA is turned ON for the PLR measurements with phase acquisition; otherwise, it is bypassed. The CPA is then followed by the RS decoder and the FPGA-based BERT.

### Burst-Mode Receiver Functionalities

The idea behind the CPA is based on the simple, fast, and effective algorithm in [108]. Since the CDR samples the data twice per bit, the odd samples and even samples (O and E, respectively in Figure 3.2b). The odd samples are forwarded to path O and the even samples to path E. The byte synchronizer is responsible for detecting the delimiter. It makes use of a payload detection algorithm to look for a preprogrammed delimiter. The idea behind the phase picking algorithm is to replicate the byte synchronizer twice in an attempt to detect the delimiter on either the odd and/or even samples of the data respectively. That is, regardless of any phase step, i.e., $-2\pi \leq \Delta\varphi \leq +2\pi$, between consecutive packets, there will be at least one clock edge (either todd or teven) that will yield an accurate sample. The phase picker then uses feedback from the byte synchronizers to select the correct path from the two possibilities. The realigned data is sent to the RS(255,239) decoder which is turned on for BER measurements with FEC, otherwise it is bypassed (Figure 3.2b). The RS decoder is an IP core from the Xilinx LogiCORE portfolio. The FPGA-based BERT designed in [108] is implemented to selectively perform BER and PLR measurements on only the

payload of the packets. The BERT compares the incoming data with an internally generated $2^{15}$-1 PRBS. This eliminates the need to up convert the frequency back to 622 Mbps or 666.43 Mbps using an 8:1 serializer after the FPGA, and avoids the use of a commercial BERT. Note that conventional BERTs require a continuous alignment between the incoming pattern and the reference pattern, and milliseconds to acquire synchronization. The phase step response of the burst-mode CDR can make conventional BERTs lose pattern synchronization at the beginning of every packet while the sampling clock is being recovered by the CDR. The custom BERT does not require fixed synchronization between the incoming pattern and the reference pattern of the error detector. Synchronization happens instantaneously at the beginning of every packet, therefore enabling PLR measurements on discontinuous, bursty data.

### 3.2. Experimental Setup and Results

The experimental setup illustrated in Figure 3.3 is used to test the uplink of the LS and CLS SAC-OCDMA PON architectures shown in Figure 3.1, using only the two-feeder topology. A single incoherent broadband source (BBS) is filtered around 1542.5 nm using two cascaded FBG band-pass filters providing a 9.6 nm band, and serves to test both the CLS and LS architectures. An NRZ 215-1 PRBS is input to a single polarization independent electro-absorption modulator (EAM) that, in conjunction with appropriate decorrelating delay lines, represents independent data streams each modulated externally at a distinct ONU. For the CLS architecture, the single powerful BBS is sent over the 20 km CLS/downlink feeder and is then split by the first 1×8 coupler representing the RN. For the LS architecture, the 20 km single mode fiber (SMF-28) is not present and the first 1×8 coupler is not part of the network, but rather an experimental trick to emulate eight separate, low power incoherent sources. The balance of the setup is interpreted as seven ONUs each with a distinct CDMA encoder, followed by the second 1×8 coupler representing the RN and a 20 km SMF for the uplink in the two-feeder

architecture. We did not use the circulators and the WDM filter in Figure 3.1, as we were only testing the uplink; these components would only contribute to insertion losses.

At the OLT an appropriate dispersion compensation fiber (DCF) is used, and the signal is amplified by an erbium-doped fiber amplifier (EDFA) and detected in a balanced receiver. A variable optical attenuator (VOA) serves to control the received power level. A balanced detection scheme similar to that in Figure 3.1 is then used to decode user 1. To ensure good detection and MAI cancellation, the optical lengths of the two branches of the receiver are perfectly adjusted; furthermore, the power at both arms due to MAI is controlled using another VOA (not shown in Figure 3.3) that accounts also for the splitting ratio of the 1×2 coupler as in [51]. After decoding, each arm goes into one of the two separate inputs of an 800-MHz balanced photodiode from New Focus (model 1617). The electrical signal is then amplified (MITEQ, 0.01–500 MHz) and low-pass filtered by a 4th order Bessel-Thomson filter (Picosecond, 467 MHz) to remove the out-of-band high-frequency electrical noise. Such a filter reduces intensity noise from the incoherent broadband source [51], while keeping inter-symbol interference to a minimum.

Measurements are then performed with either a global clock, or through our OCDMA burst-mode receiver, corresponding to switch position 1 or 2, respectively. The desired information rate per user is 622 Mbps; an RS(255,239) code introducing 15/14 overhead leads to an aggregate bit rate of 666.43 Mbps. The spectral coding is achieved by FBGs working in transmission; balanced incomplete block design (BIBD) codes with length 7 and weight 3 are used as in [51].

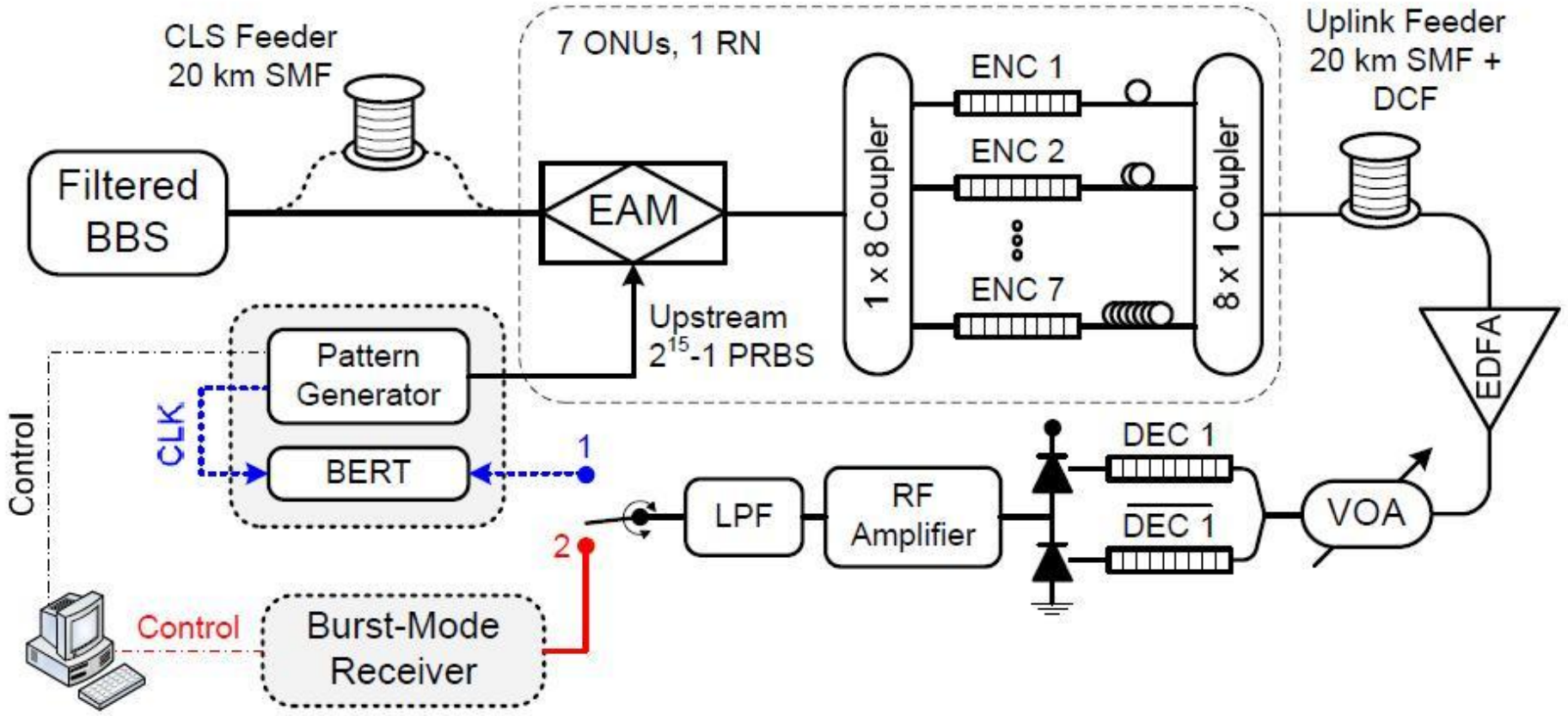


Figure 3.3. Experimental setup for a 7×622 Mbps SAC-OCDMA PON uplink (BERT: BER tester, CLK: clock, DEC: decoder, and ENC: encoder).

## Results and Discussions

In this subsection we present the system performance in terms of BER, PLR and the CID immunity for the back-to-back configuration (without fiber link), and the LS and the CLS SAC-OCDMA PON architectures. The experimental results are presented in Figure 3.4 and Figure 3.5 which shows simulation versus measurement results.

We present also the power and link budget for the different architectures that were tested. BER measurements are reported for continuous upstream traffic, while PLR is reported for packet data, based on the burst-mode BERT results. PLR measurements use bursty traffic (similar to that in Figure 3.2a) with packets of $2^{15}$-1 bits length and zero preamble length; use of a preamble would improve PLR, but at the cost of reduced throughput. Today's PON standards provide for a maximum preamble length of 28 bits [51], to allow the receiver enough time to recover the clock, adjust the phase, and control the gain.

For easier comparison of the back-to-back configuration and the two PON architectures, we plot in Figure 3.4 the single user and fully loaded (seven users) systems BER curves. We consider the performance using our burst-mode receiver when the FEC module is OFF (curves with unfilled markers), and when it is ON (curves with filled markers). A coding gain of more than 2.5 dB (measured at BER = $10^{-9}$) is observed for a single user for the three architectures. Furthermore, the penalty from a back-to-back configuration to the LS PON is negligible (less than 0.25 dB), as well as the one from a LS PON to the CLS PON architecture. Results are consistent with that in [52] for a back-to-back configuration and a 20 km communication link. For the seven users case, we see clearly

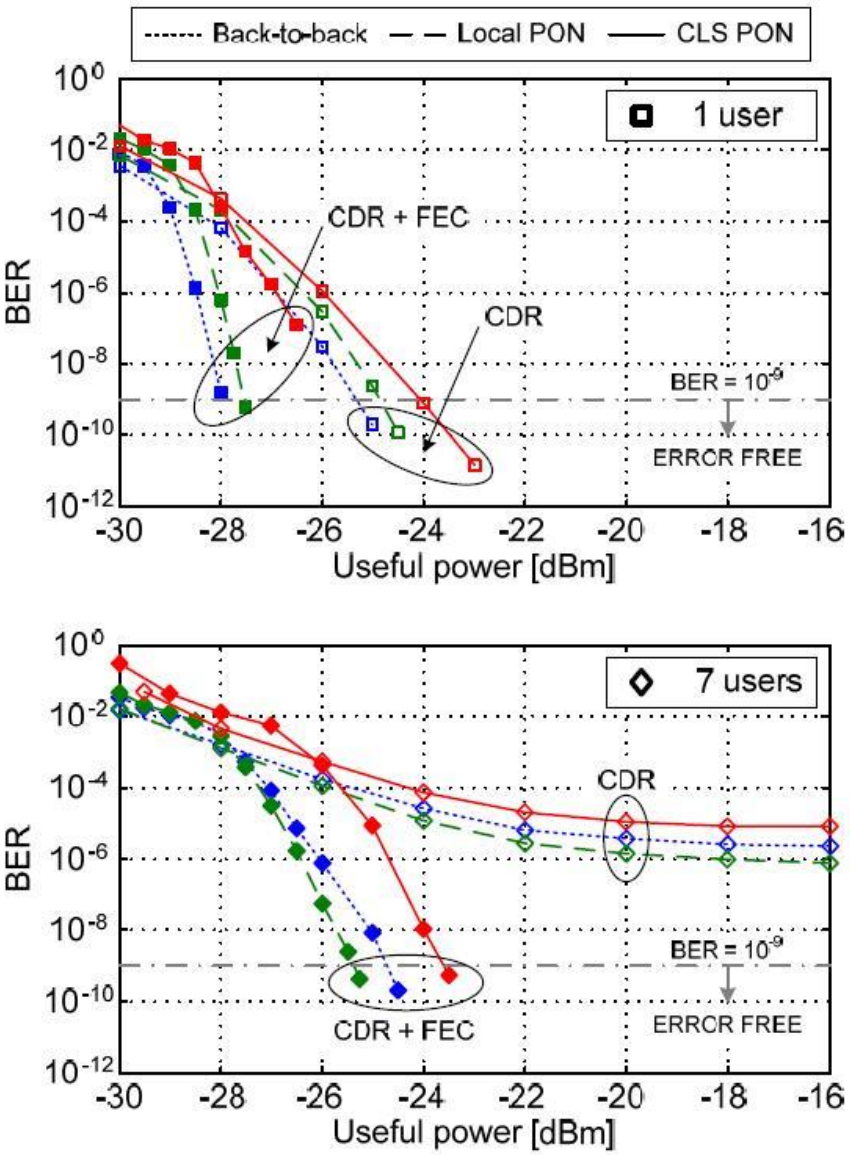


Figure 3.4. BER vs. useful power for a single user and fully-loaded systems (Dotted lines for back-toback; dashed lines for LS architecture; solid lines for CLS architecture).

all BER floors are eliminated by the FEC. Operating at a relatively low power (-23 dBm received power) we obtain error free transmission (BER << $10^{-9}$) for the three architectures. Therefore, we were able to demonstrate for the first time to our knowledge an error free 7×622 Mbps uplink of an incoherent SAC-OCDMA PON (LS and CLS architectures were tested) using a standalone burst-mode receiver with CDR and FEC. Finally, in Figure 3.4 we can compare the performance of LS and CLS architectures under our assumption of an 8:1 ratio of the relative power of the centralized to the local sources. A penalty of less than 2

dB was measured for LS at a bit error rate (BER) of $10^{-9}$ when FEC and CDR were in use. Recall that this penalty is for the particular instance of a network of eight users, and an 8:1 ratio of relative power. We will discuss later how to generalize these results.

Simulation versus measurement of the BER using FEC for the three different configurations is shown in Figure 3.5. Organizing the bits in symbols of m bits yields an equivalent symbol error rate of

$$P_s = 1 - (1 - P_B)^m \tag{3.1}$$

The RS(255,239) FEC uses 8 bit symbols and, in a memoryless channel, can correct up to t = 8 symbol errors per frame (239 uncoded symbols), yielding a symbol error rate after FEC of [110]

$$P_{S_{FEC}} \approx \frac{1}{2^m - 1} \sum_{j=t+1}^{2^m-1} j \binom{2^m - 1}{j} P_S^j (1 - P_S)^{2^m - 1 - j} \tag{3.2}$$

Again assuming a memoryless channel, the bit error rate $P_{B\_FEC}$ is about one half this symbol error rate, as we are using orthogonal signaling (on-off keying). We plot the memoryless channel prediction for PB_FEC and our measurement in Figure 3.5. There is one order of magnitude mismatch between simulation and measurements; our predictions are too optimistic. This is more likely due to the memory added to the channel through the BBS (intensity noise), the CDR, and other components.

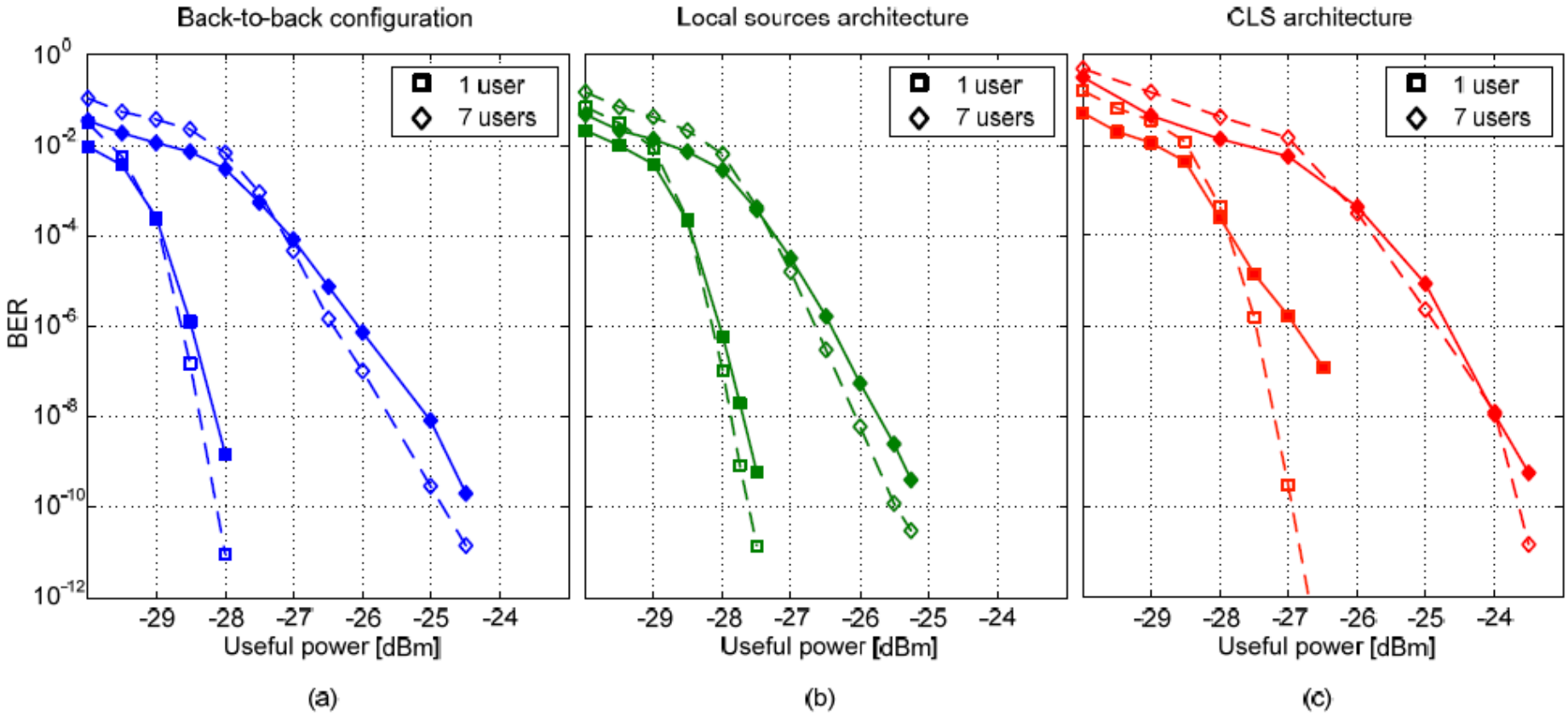


Figure 3.5. Simulated and measured BER vs. useful power for different configurations (Dashed lines for simulated BER; solid lines for measurements).

### 3.3. Impact of PON Size on Local Sources versus CLS PON Architectures

In this section we examine the relative merits (cost and performance) of local sources versus centralized architectures. The power budget of a PON is an important parameter in the design, as it helps FTTH service providers to select the appropriate light sources and the convenient receivers for their network. The power budget is mainly determined from the PON physical architecture. The uplink power budget of the CLS architecture ($P_{Budget,CLS}$) is related to that of the LS architecture ($P_{Budget,LS}$) by the following equation:

$$P_{Budget,CLS} = 10\log\left(\frac{P_{CLS}}{P_{LS}}\right) - 10logN - \alpha_F D + P_{Budget,LS} \qquad (3.3)$$

where, $P_{CLS}$ and $P_{LS}$ are the source power for CLS and LS architectures, respectively, N is the number of splits (or number of ONUs), $\alpha_F$ is the fiber attenuation in dB/km, and D is the feeder length in km. The first term in (3.3) represents the gain in relative power that can be achieved in CLS architectures; we expect $P_{CLS}$ to be much greater than PLS. The second and third terms represent the extra splitting losses and additional fiber attenuation in CLS architectures, respectively. In CLS architectures an EDFA can be used at the central office to increase the margin by compensating the extra losses terms in (3.3).

Using a semiconductor optical amplifier (SOA) or a reflective SOA at ONU for modulation instead of the EAM reduces the amplification requirements in both architectures. Placing a gain saturated SOA at the central office can further reduce the intensity noise of BBS as in spectrum-sliced WDM PONs. The possibility of integration of the external modulators (using silicon) can be advantageous from the cost point of view. The selection of a powerful light source for CLS PONs also increases the power budget as in (3.3). The cumulative cost of light sources in LS architectures is N times the cost of a single local source, and this should be compared to the cost of the single high power source for the CLS solutions. Using powerful directly modulated LEDs at 622 Mbps could tilt costs in favor of LS architectures by eliminating the need for modulators. However, these super-

luminescent

Table 3.1.

Uplink power budget and link loss for both PON architectures.

| | LS | LS(Effective) | CLS |
|---|---|---|---|
| Source Power $[dBm]$ | 2.83 | -6.62 | .83 |
| RN Splitting | 18.88 | 9.43 | 18.88 |
| ODN Feeders | 3.95 | 3.95 | .07 |
| Loss $[dB]$ Modulation | 12.20 | 12.20 | 14.51 |
| Encoding | 3.99 | 3.99 | .99 |
| DCF | 2.41 | 2.41 | .41 |
| Decoding | 6.42 | 6.42 | .42 |
| Total Loss | 47.85 | 38.40 | 51.28 |
| Amplification $[dB]$ | 36.56 | 36.56 | 0.84 |
| Received Power $[dBm]$ | 8.46 | -8.46 | 7.61 |

LEDs have cost comparable to that of the BBS we used, and they require temperature control.

Table 3.1 details the uplink power budget and optical losses in our

experimental realization of the two SAC-OCDMA PON architectures. In the column marked LS (effective) we give the values when interpreting the combination of the BBS and the first 1×8 splitter (see Figure 3.3) as eight independent sources for each of the ONUs. Effectively, the total losses in the LS configuration was approximately 39 dB (excluding 9 dB losses through the 1×8 splitter incurred for experimental convenience), whereas the total losses in a similar CLS PON was roughly 52 dB. The 13 dB difference is the contribution of the extra 9 dB losses of the 1×8 coupler on the CLS first passing through RN before modulation, and the extra 4 dB losses for the unmodulated light traversing 20 km of SMF. For our experiment, examining the final two columns of Table 3.1, $P_{Budget,CLS}$= -48.45 dBm (excluding amplification), $P_{Budget,LS}$= -45.02 dBm (excluding amplification). Note that $P_{CLS}$ /$P_{LS}$ was chosen to offset the RN losses of 10logN dB, so the only remaining difference was the additional fiber losses.

The second 8×1 coupler in Figure 3.1a represents the splitting loss at the RN. From Table 3.1, the RN splitting losses represent the major source of losses, and would be higher for larger PONs with 1:32 or 1:64 splitting ratio. Fiber losses are the combinations of propagation losses (20 km and 40 km of SMF-28 for LS and CLS architectures, respectively), and a 2.41 dB loss DCF. The modulation losses for the CLS PON is greater than that of the local sources, as the input power to the modulator is lower (see Figure 3.3); the light travels a 20 km feeder before it reaches the ONU. Encoding and decoding losses are related to the design of the codes and FBGs, namely, the code weight and the reflectivity of each frequency bin. The decoding losses shown in Table 3.1 include also a 3.5 dB loss of the 1×2 coupler at the balanced receiver. Modulation and encoding/decoding losses should remain almost the same for larger PONs. Because the EDFAs are not gain clamped, we note that the gain varies from one configuration to the other depending on the corresponding EDFA input power. The maximum received power levels for both architectures are illustrated in Table 3.1; recall that at -23 dBm we achieve error free operation for the two PON architectures. Practically, the gain of the EDFAs, as well as the source power, must be sufficient to overcome

the losses and the limited sensitivity of the receiver. Using avalanche photodetectors (APD), for example, increases the link margin.

Extrapolating our results for larger PONs using (3.3), we note that in CLS architectures the loss budget goes up with the square of the number of splits, instead of being proportional to the number of splits for the LS solution. In other words, doubling the number of users in a LS architecture imposes an additional 3 dB loss, whereas for CLS PONs there is a 6 dB extra loss. The same relationship holds when increasing the PON physical reach. However, as discussed earlier this extra loss can be compensated using amplification at the OLT, or SOAs at the ONUs, without increasing the cost significantly.

## Summary

We proposed and experimentally demonstrated different incoherent SAC-OCDMA PON physical architectures using a standalone burst-mode receiver at the OLT side. Local sources and centralized sources architectures have been examined. For experimental convenience, we examined only the two-feeder architecture; therefore, the effects of Rayleigh back-scattering are not addressed. Continuous and bursty upstream traffic for seven asynchronous users at 622 Mbps were considered for the BER and the PLR.

Concerning OCDMA for future PONs, we proposed and experimentally demonstrated the uplink of a 7×622 Mb/s SAC-OCDMA PON with burst-mode operation. Both LS and CLS architectures were considered, and examined over a 20 km link (with DCF). Extra splitting and propagation losses exist for CLS architectures as the uplink signal travels through the network back and forth. A power penalty of less than 2 dB was measured at a BER of $10^{-9}$ under certain assumptions on the relative power of the sources. We showed that the selection of the appropriate light sources plays an important role in the power budget, and can help increase the link margin. Using a Reed-Solomon RS(255,239) FEC, a coding gain of 2.5 dB was reported for a single-user system, and error free transmission (BER < $10^{-9}$) was achieved for a fully loaded PON for the two architectures. Due to a CPA algorithm, even with zero preamble bits we report a zero PLR for up to

four simultaneous users, and more than two orders of magnitude improvement in the PLR for a fully loaded PON.

Despite the good results we obtained for our SAC-OCDMA solution, the power budget was critical and therefore OLT amplification was required even for LS architectures. Putting aside the splitting losses at the RN, the use of an external modulator, together with the OCDMA encoding and decoding contributed to more than 20 dB of losses. SSWDM (i.e., incoherent WDM) can support the same number of users as SAC-OCDMA for the same number of frequency bins; therefore, there is no advantage for SAC-OCDMA over SS-WDM in terms of capacity.

# 4. SAFETY ENGINEERING

## 4.1. General requirements of safety engineering during the work with personal computer

Requirements of work security, that are set forth here, are assigned on personal, that operating personal computers, programmers, PC users, who combines the work of operator with main work on PC less than their working time. Normal daily duration of the work time is eight hours, i.e. forty hours in week with two vacation days in Saturday and Sunday.

For the guaranteeing of optimal capacity for work and maintenance of health of professional users regulated breaks must be ranged during the working shift. Time of regulated breaks during the working shift is settled according to her duration, type and category of the work activity.

Duration of continuous work with PC without regulated breaks must not exceed two hours. During the eight and twelve hourly working shift regulated breaks are settled by fifteen minutes after every work hour.

During the work with PC in a night shift (from 1- p.m. hours to 6 a.m.), regardless of category and type of working activity, regulated breaks duration is exceeded to sixty minutes.

During regulated breaks for reduction of emotional stress, tiredness of visual analyzer, suppression of hypodynamia and hypokinesia influence, prevention of fatigue development personal must execute special training complexes.

If personal, that works with PC, has visual discomfort and other inauspicious feelings, insipid of maintenance of sanitary and hygienic, ergonomic requirements, work modes and vacation it’s necessary to use individual approach in limiting the work time with PC, correction of break duration for vacation or change the working activity on other, that not associated with using PC.

During the work PC’s user contacts with dangerous and harmful production factors (DHPF). Dangerous production factor is the factor, which’s influence on the personal, in the definite conditions, could lead to injury or suddenly health worsening, degradation or illness.

During the work process PC’s user confronts with next DHPF.

Physical:

- increased electromagnetic radiation levels
- increased X-ray radiation levels
- increased ultraviolet radiation levels
- increased infrared radiation level
- increased static electricity level
- increased suspended materials concentration level in the working zone
- increased air ion maintenance in the air of the working zone
- decreased negative air ion maintenance in the air of the working zone
- decreased of increased air moisture
- decreased of increased air mobility of the working zone
- increased noise level
- decreased of increased consecration level
- increased straight brightness level
- increased reflected brightness level
- increased blindness level
- brightness distribution irregularity in the field of vision
- increased light image brightness
- increased light flux pulsation level
- increased voltage significance in electric chain, which’s locking could pass throw the human body

Chemical:

- increased carbon dioxide, ozone, ammonia, phenol, formaldehyde and polychloride biphenyl maintenance in the air of the working zone

Psychophysiological:

- sustained statical load
- stereotyped working motions
- intellectual overstrain
- monotonous load

- sensory loads
- vision strain
- attention strain
- big information capacity, which processed in the unit time
- work mode

Irrational working place organization

Biological:

- increased microorganism maintenance in the air of the working zone

Contact with DHPF could bring to injuries or different illness development, that affects cardiovascular, respiratory, nervous systems, liver, kidney and so on. Pregnant women do not admitted to implementation of all kinds of works, that concerned with PC using since pregnancy's ascertainment and in the baby breast-feeding period.

PC user should use individual protection facilities:

Preventive devices, display guard filter of the "absolute protection" grade, spectral glasses, implementation of the personal hygiene rules.

### 4.2. Requirements of safety before the work with PC

1. Inspect and put to rights the working place.
2. Adjust consecration on the working place, make sure in enough consecration, in absence of the reverberation on the screen, in absence of the counter light flux.
3. Check the equipment connection propriety in the electricity supply.
4. Make sure in the protective ground presence and screenful conductor connection to the processor case.
5. To wipe the screen surface and the guard filter with a special napkin.
6. Make sure in absence of the floppy disks in the disk drives of the PC processor.
7. Check the precision of the table arrangement, legs pedestal, equipment position, screen tilt angle, keyboard position, and, if it's necessary, carry out the regulation of the working table and the armchair, PC elements arrangement in accordance with ergonomics demands for the purpose of uncomfortable poses and long body tiredness exception.

8. During the turning on PC's user must obey the next engaging equipment consecution:
9. Turn on the power unit.
10. Turn on the peripheral device (printer, monitor, scanner and so on)
11. Turn on the system case. (processor)
12. PC's user doesn't allowed to begin the work in view of:
13. Information absence of conditions of work attestation results on the present working place or in the presence of information of present equipment parameters discrepancy to sanitary standard demands.
14. Display guard filter of the "absolute protection" grade absence.
15. Disconnect ground conductor of the guard filter.
16. Equipment faultiness detection.
17. Guard ground PC device absence.
18. Carbon-dioxide or powder-type fire extinguisher and first-aid kit absence.
19. Hygienic regulations PC disposal violation.

### 4.3. Safety engineering during the work with personal computer

During the work PC user must:

- keep in clean and proper the working place during the whole of working day.
- open all device vent ducts.
- use "mouse" in the presence of special pad.
- correctly close all active tasks.
- Power off the power supply only in that case, if operator during the breaks after the PC work should to be near the display terminal (less than 2 m), otherwise you can not power off the power supply.
- execute the sanitary code and observe the routines of work and rest.
- Observe the computer engineering exploitation rules in accordance with exploitation direction.
- During the work with text information you must choose physiological

view mode of black symbols on the white background.

- According to daily time-table make up the eyes, neck, arms, body and legs relaxation.
- Observe the distance between the eyes and monitor in the range of 60-80 sm.

During the work PC user isn't allowed:

- Touch the monitor and the keyboard at the same time; touch the back panel of the system case (processor) at powered conditions.
- Switch the peripheral devices interface cable at powered conditions.
- Put the paper and other items under the top panel.
- Admit the disarrange of the working place with paper for the purpose of barring accumulation of organic dust.
- Switch off during the executing the active task.
- Make the frequent power switches.
- Let the ingress of moisture on the system case(processor) surface, monitor, keyboard working zone disk drives, printers and other devices.
- Power on the strongly chilled devices.
- Perform the opening and repairing the devices unassisted.

**Summary**

Requirements of work security, that are set forth here, are assigned on personal, that operating personal computers, programmers, PC users, who combines the work of operator with main work on PC less than their working time. Normal daily duration of the work time is eight hours, i.e. forty hours in week with two vacation days in Saturday and Sunday.

# CONCLUSION

Goal of the thesis is to implement optical code division multiple access and study its impairments and solutions.

Chapter 1 outlines the motivation for the development of optical communication networks. Various multiplexing techniques that can be used to increase the capacity of an optical network are outlined. Network topologies are discussed with particular interest given to access networks. Within this section, current forms of electrical access networks are discussed with the problems facing these networks also highlighted. Various forms of optical access networks are then presented with attention given to an emerging network that gained significant interest in research; an optical code division multiple access network.

Chapter 2 focuses on the multiplexing technique of optical code division multiple access (OCDMA). The various methods proposed for optical encoding and decoding of a signal in an OCDMA network are presented. The advantages and disadvantages associated with each are also discussed. Since the performance of an OCDMA system relies on the optical codes used, the various forms of optical codes that have been presented in relation to this multiplexing technique are also discussed. OCDMA systems suffer from two major network impairments that can severely limit the capacity of the system. The source of these impairments is examined while experimentally demonstrated techniques for the removal of such noise sources are also explored.

The experimental results are considered in chapter 3. We proposed and experimentally demonstrated different incoherent SAC-OCDMA PON physical architectures using a standalone burst-mode receiver at the OLT side. Local sources and centralized sources architectures have been examined. For experimental convenience, we examined only the two-feeder architecture; therefore, the effects of Rayleigh back-scattering are not addressed. Continuous and bursty upstream traffic for seven asynchronous users at 622 Mbps were considered for the BER and the PLR.

Concerning OCDMA for future PONs, we proposed and experimentally

demonstrated the uplink of a 7×622 Mb/s SAC-OCDMA PON with burst-mode operation. Both LS and CLS architectures were considered, and examined over a 20 km link (with DCF). Extra splitting and propagation losses exist for CLS architectures as the uplink signal travels through the network back and forth. A power penalty of less than 2 dB was measured at a BER of $10^{-9}$ under certain assumptions on the relative power of the sources. We showed that the selection of the appropriate light sources plays an important role in the power budget, and can help increase the link margin. Using a Reed-Solomon RS(255,239) FEC, a coding gain of 2.5 dB was reported for a single-user system, and error free transmission (BER < $10^{-9}$) was achieved for a fully loaded PON for the two architectures. Due to a CPA algorithm, even with zero preamble bits we report a zero PLR for up to four simultaneous users, and more than two orders of magnitude improvement in the PLR for a fully loaded PON.

## USED LITERATURE

1. Decree of President of the Republic Uzbekistan 21.03.2012 y. N PP-1730 "О мерах по дальнейшему внедрению и развитию современных информационно-коммуникационных технологий"

2. H. G. Weber, S. Ferber, M. Kroh, C. Schmidt-Langhorst, R. Ludwig, V. Marembert, C. Boerner, F. Futami, S. Watanabe, and C. Schubert, "Single channel 1.28 Tbit/s and 2.56 Tbit/s DQPSK transmission," Electronics Letters, vol. 42, no. 3, pp. 178–179, 2006.

3. H.-G. Weber, R. Ludwig, S. Ferber, C. Schmidt-Langhorst, M. Kroh, V. Marembert, C. Boerner, and C. Schubert, "Ultrahigh-speed OTDM-transmission technology," IEEE Journal of Lightwave Technology, vol. 24, no. 12, pp. 4616–4627, 2006.

4. R. Ludwig, S. Diez, A. Ehrhardt, L. Kueller, W. Pieper, and H. G. Weber, "A tunable femtosecond modelocked semiconductor laser for applications in OTDM-systems," IEICE Transactions on Electronics, vol. E81-C, no. 2, pp. 140–145, 1998.

5. M. D. Pelusi, Y. Matsui, and A. Suzuki, "Femtosecond optical pulse generation from an electro-absorption modulator with repetition rate and wavelength tuning," in Proceedings of European Conference on Optical Communications (ECOC), Nice, France, 1999, pp. 26–27.

6. H. Murai, M. Kagawa, H. Tsuji, and K. Fujii, "EA-modulator-based optical time division multiplexing/demultiplexing techniques for 160-Gb/s optical signal transmission," IEEE Journal of Selected Topics in Quantum Electronics, vol. 13, no. 1, pp. 70–78, 2007.

7. S. L. Jansen, M. Heid, S. Splater, E. Meissner, C. J. Weiste, A. Schopflin, D. Khoe, and H. De Waarth, "Demultiplexing 160 Gb/s OTDM signal to 40 Gb/s by FWM in an SOA," Electronics Letters, vol. 38, no. 17, pp. 978–980, 2002.

8. J. P. Sokoloff, P. R. Prucnal, I. Glesk, and M. Kane, "A terahertz optical asymmetric demultiplexer (TOAD)," IEEE Photonics Technology Letters, vol. 5,

no. 7, pp. 787– 790, 1993.

9. H. T. Yamada, H. Murai, A. R. Pratt, and Y. Ozeki, “Scalable 80 Gb/s OTDM using a modular architecture based on EA modulators,” in Proceedings of European Conference on Optical Communications (ECOC), Munich, Germany, 2000, paper P3.31.

10. J. Slovak, T. Tekin, C. Bornholdt, B. Sartorius, E. Lach, M. Schmidt, S. Vorbeck, and R. Leppla, “Self-pulsating laser based all-optical clock recovery applied in 421 km field experiment for 170.6 : 42.7 Gbit/s OTDM demultiplexing,” in Proceedings of European Conference on Optical Communications (ECOC), Glasgow, Scotland, 2005, paper Th. 3.1.3.

11. E. Lach, K. Schuh, M. Schimdt, B. Junginger, G. Charlet, P. Pecci, and G. Veith, “7 _ 170 Gbits/s (160 Gbits/s + FEC overhead) DWDM transmission with 0.53 bit/s/Hz spectral efficiency over long haul distance of standard SMF,” in Proceedings of European Conference on Optical Communications (ECOC), Rimini, Italy, 2003, pp. 68–69.

12. L. M¨oller, Y. Su, X. Liu, J. Leuthold, and C. Xie, “Generation of 160 Gb/s carriersuppressed return-to-zero signals,” in Proceedings of European Conference on Optical Communications (ECOC), Remini, Italy, 2003, pp. 50–51.

13. S. Feber, R. Ludwig, C. Boerner, A. Wietfield, B. Schmauss, J. Berger, C. Schubert, G. Unterboersch, and H. G. Weber, “Comparision of DPSK and OOK modulation format in 160 Gb/s transmission system,” in Proceedings of European Conference on Optical Communications (ECOC), Remini, Italy, 2003, pp. 1004–1005.

14. M. J. O’Mahony, “Optical multiplexing fibre networks: Progress in WDM and OTDM,” IEEE Communications Magazine, vol. 33, no. 12, pp. 82–88, 1995.

15. B. Nyman, M. Farries, and C. Si, “Technology trends in dense WDM demultiplexers,” Optical Fiber Technology, vol. 7, no. 4, pp. 255–274, 2001.

16. T. Li, “The impact of optical amplifiers on long-distance lightwave telecommunications,” Proceedings of the IEEE, vol. 81, no. 11, pp. 1568–1579, 1993.

17. J. Kani, K. Hattori, M. Jinno, T. Kanamori, and K. Oguchi, “Triple-wavelength-band WDM transmission over cascaded dispersion-shifted fibers,” IEEE Photonics Technology Letters, vol. 11, no. 11, pp. 1506–1508, 1999.
18. International Telecommunications Union, “ITU-T recommendation G.694.1 spectral grids for WDM applications: DWDM applications,” Series G: Transmission systems and media, digital systems and networks, vol. Transmission media characteristics- Characteristics of optical components and subsystems, no. G.694.1, 2002.
19. G.Varaille and J. F.Marcerou, “1.8 Tbit/s 6500 km transoceanic NRZ system assessment with industrial margins using 25 GHz channel spacing,” in Proceedings of European Conference on Optical Communications (ECOC), Copenhagen, Denmark, 2002, paper 9.1.3.
20. H. Suzuki, M. Fujiwara, and K. Iwatsuki, “Application of super-DWDM technologies to terrestrial terabit transmission systems,” IEEE Journal of Lightwave Technology, vol. 24, no. 5, pp. 1998–2005, 2006.
21. S. Kuwahara, A. Hirano, Y. Miyamoto, and K. Murata, “Automatic dispersion compensation for WDM system by mode-splitting of tone-modulated CS-RZ signal,” in Proceedings of European Conference on Optical Communications (ECOC), Copenhagen, Denmark, 2002, paper 6.1.3.
22. M. Schmidt, M. Witte, F. Buchali, E. L. andE. Le Rouzic, S. Salaun, S. Vorbeck, and R. Leppla, “8 _ 170 Gb/s DWDM field transmission experiment over 430 km SSMF using adaptive PMD compensation,” in Proceedings of European Conference on Optical Communications (ECOC), Stockholm, Sweden, 2004, paper Th4.1.2.
23. J. Berthold, A. A. M. Saleh, L. Blair, and J. M. Simmons, “Optical networking: Past, present, and future,” IEEE Journal of Lightwave Technology, vol. 26, no. 9, pp. 1104– 1118, 2008.
24. G. R. Cooper and R. W. Nettleton, “A spread spectrum technique for high capacity mobile communications,” IEEE Transactions on Vehicular Technology, vol. 27, no. 4, pp. 264–275, 1978.

25. H. J. Kochevar, “Spread spectrum multiple access communication experiment through a satellite,” IEEE Transactions on Communications, vol. 25, no. 8, pp. 853–856, 1977.

26. H. Sotobayashi,W. Chujo, and K. Kitayama, “Highly spectrally-efficient optical codedivision multiplexing transmission system,” IEEE Journal of Selected Topics in Quantum Electronics, vol. 10, no. 2, pp. 250–258, 2004.

27. X. Wang and K. Kitayama, “Analysis of beat noise in coherent and incoherent timespreading OCDMA,” IEEE Journal of Lightwave Technology, vol. 22, no. 10, pp. 2226–2235, 2004.

28. D. D. Sampson, G. J. Pencock, and R. A. Griffin, “Photonic code-division multipleaccess communications,” Fiber and Integrated Optics, vol. 16, no. 2, pp. 129–157, 1997.

29. K. Grobe and J.-P. Elbers, “PON in adolescence: From TDMA to WDM-PON,” IEEE Communications Magazine, vol. 46, no. 1, pp. 26–34, 2008.

30. C.-H. Lee,W. V. Sorin, and B. Y. Kim, “Fiber to the home using a PON infrastructure,” IEEE Journal of Lightwave Technology, vol. 24, no. 12, pp. 4568–4583, 2006.

31. C.-H. Lee, S.-M. Lee, K.-M. Choi, J.-H. Moon, S.-G. Mun, K.-T. Jeong, J. H. Kim, and B. Kim, “WDM-PON experiences in Korea,” Journal of Optical Networking, vol. 6, no. 5, pp. 451–464, 2007.

32. W. Mao, P. A. Andrekson, and J. Toulousse, “Investigation of a spectrally flat multiwavelength DWDM source based on optical phase- and intensity-modulation,” in Proceedings of Optical Fibre Communications (OFC), Los Angeles, California, 2004, paper MF78.

33. P. Healy, P. Townsend, C. Ford, L. Johnston, P. Townley, I. Lealman, L. Rovers, S. Perrin, and R. Moore, “Spectral slicing WDM-PON using wavelength-seeded reflective SOAs,” Electronics Letters, vol. 37, no. 19, pp. 1181–1182, 2001.

34. P. R. Prucnal, M. A. Santoro, and T. R. Fan, “Spread spectrum fiber-optic local area network using optical processing,” IEEE Journal of Lightwave Technology, vol. LT-4, no. 5, pp. 547–554, 1986.

35. X. Wang, K. Matsushima, A. Nishiki, N. Wada, F. Kubota, and K.-I. Kitayama, "Experimental demonstration of 511-chip 640 Gchip/s superstructured FBG for high performance optical code processing," in Proceedings of European Conference on Optical Communications (ECOC), Stockholm, Sweden, 2004, paper Tu1.3.7.

36. Z. Jiang, D. S. Seo, S.-D. Yang, D. E. Leaird, R. V. Roussev, C. Langrock, M. M. Fejer, and A. M.Weiner, "Four-user, 2.5-Gb/s, spectrally coded OCDMA system demonstration using low-power nonlinear processing," IEEE Journal of Lightwave Technology, vol. 23, no. 1, pp. 143–158, 2005.

37. X. Wang, N. Wada, T. Hamanaka, K. Kitayama, and A. Nishiki, "10-user, trulyasynchronous OCDMA experiment with 511-chip SSFBG en/decoder and SC-based optical thresholder," in Proceedings of Optical Fibre Communications (OFC), Anaheim, California, 2005, postdeadline paper PDP33.

38. A. Stok and E. H. Sargent, "The role of optical CDMA in access networks," IEEE Communications Magazine, vol. 40, no. 9, pp. 83–87, 2002.

39. J. Wu, F. R. Gu, and H.-W. Tsao, "Jitter performance analysis of SOCDMA-based EPON using perfect difference codes," IEEE Journal of Lightwave Technology, vol. 22, no. 5, pp. 1309–1319, 2004.

40. X. W. Ken-Ichi Kitayama and N. Wada, "OCDMA over WDM-PON-solution path to gigabit-symmetric FTTH," IEEE Journal of Lightwave Technology, vol. 24, no. 4, pp. 1654–1662, 2006.

41. R. P. Scott, V. J. Hernandez, N. K. Fontaine, F. M. Soares, R. Broeke, K. Perry, G. Nowak, C. Yang, W. Cong, K. Okamoto, B. H. Kolner, J. P. Heritage, and S. J. B. Yoo, "80.8-km BOSSNET SPECTS O-CDMA field trial using subpico second pulses and a fully integrated, compact AWG-based encoder/decoder," IEEE Journal of Selected Topics in Quantum Electronics, vol. 13, no. 5, pp. 1455–1462, 2007. 24

42. G. R. Cooper and R. W. Nettleton, "A spread spectrum technique for high capacity mobile communications," IEEE Transactions on Vehicular Technology, vol. 27, no. 4, pp. 264–275, 1978.

43. H. J. Kochevar, “Spread spectrum multiple access communication experiment through a satellite,” IEEE Transactions on Communications, vol. 25, no. 8, pp. 853–856, 1977.

44. L. B. Milstein, “Interference rejection techniques in spread spectrum communications,” Proceedings of the IEEE, vol. 76, no. 6, pp. 657–671, 1988.

45. K. S. Gilhousen, I. M. Jacobs, R. Padovani, A. J. Viterbi, L. A. Weaver, Jr., and C. E. Wheatley, III, “On the capacity of a cellular CDMA system,” IEEE Transactions on Vehicular Technology, vol. 40, no. 2, pp. 303–312, 1991.

46. J. P. Heritage and A. M. Weiner, “Advance in spectral optical code-division multipleaccess communications,” IEEE Journal of Selected Topics in Quantum Electronics, vol. 13, no. 5, pp. 1351–1369, 2007.

47. P. R. Prucnal, M. A. Santoro, and T. R. Fan, “Spread spectrum fiber-optic local area network using optical processing,” IEEE Journal of Lightwave Technology, vol. LT-4, no. 5, pp. 547–554, 1986.

48. A. M.Weiner, J. P. Heritage, and J. A. Salehi, “Encoding and decoding of femtosecond pulses,” Optics Letters, vol. 13, no. 4, pp. 300–302, 1988.

49. D. Zaccarin and M. Kavegard, “An optical CDMA system based on spectral amplitude encoding of an LED,” IEEE Photonics Technology Letters, vol. 5, no. 4, pp. 479–482, 1993.

50. L. Tancevski and I. Andonovic, “Wavelength hopping/time spreading code division multiple access systems,” Electronics Letters, vol. 30, no. 17, pp. 1388–1390, 1994.

51. N.Wada and K. Kitayama, “A 10Gb/s optical code division multiplexing using 8-chip optical bipolar code and coherent detection,” IEEE Journal of Lightwave Technology, vol. 17, no. 10, pp. 1758–1765, 1999.

# APPLICATIONS

# THE PRESENTATION SLIDES